



GEOLOGY OF THE INTERMOUNTAIN WEST

an open-access journal of the Utah Geological Association

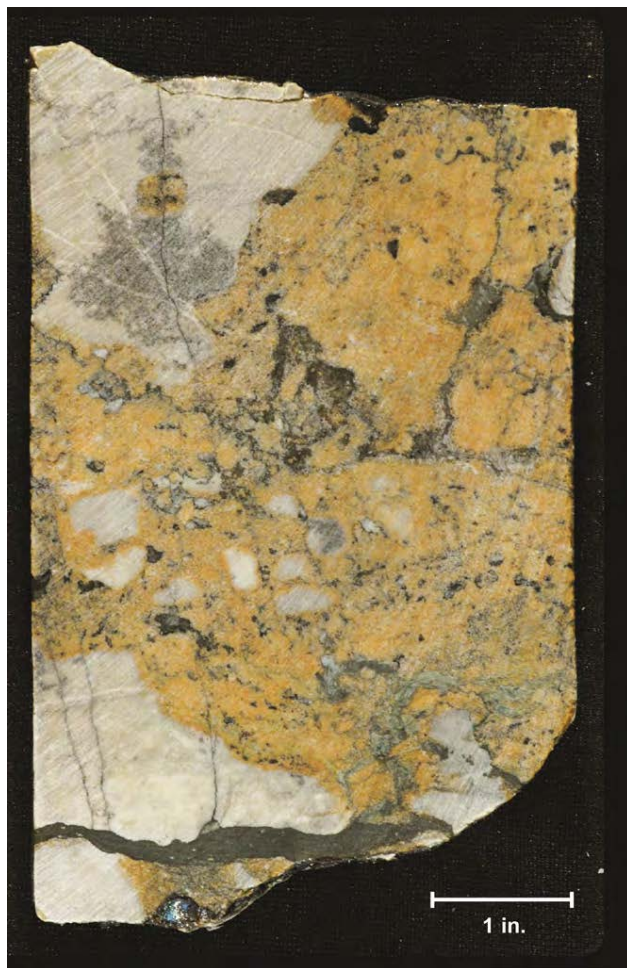
ISSN 2380-7601

Volume 7

2020

A TALE OF TWO BRECCIA TYPES IN THE MISSISSIPPIAN LEADVILLE LIMESTONE OF LISBON AND OTHER FIELDS, PARADOX BASIN, SOUTHEASTERN UTAH

Thomas C. Chidsey, Jr., David E. Eby, and Douglas A. Sprinkel





GEOLOGY OF THE INTERMOUNTAIN WEST

an open-access journal of the Utah Geological Association

ISSN 2380-7601

Volume 7

2020

Editors

Douglas A. Sprinkel Azteca Geosolutions 801.391.1977 GIW@utahgeology.org dsprinkel@gmail.com	Thomas C. Chidsey, Jr. Utah Geological Survey 801.537.3364 tomchidsey@utah.gov
Bart J. Kowallis Brigham Young University 801.380.2736 bkowallis@gmail.com	John R. Foster Utah Field House of Natural History State Park Museum 435.789.3799 eutretauranosuchus@gmail.com
Steven Schamel GeoX Consulting, Inc. 801.583-1146 geox-slc@comcast.net	

Production

Cover Design and Desktop Publishing
Douglas A. Sprinkel

Cover

Left: Cave breccia consisting of large, poorly sorted, white angular clasts of fractured limestone (or dolomite) surrounded by a yellowish altered matrix of feldspathic and granitic conglomerate and sandstone. Note also the greenish clay and black bitumen. Leadville Limestone, Big Flat No. 2 well, Grand County, Utah; slabbed core from 7630.5 feet (2325.8 m). Right: "Autobreccia" due to probable natural hydrofracturing showing a dolomite in which the "clasts" have moved very little; the black material surrounding the in-place clasts is composed of porous, late replacement dolomite coated with black bitumen. Leadville Limestone, Lisbon NW USA No. B-63 well, San Juan County, Utah; slabbed core from 9938.3 feet (3029.2 m).



This is an open-access article in which the Utah Geological Association permits unrestricted use, distribution, and reproduction of text and figures that are not noted as copyrighted, provided the original author and source are credited.

UGA Board

2020 President	Leslie Heppler	lheppler@utah.gov	801.538.5257
2020 President-Elect	Riley Brinkerhoff	riley.brinkerhoff@gmail.com	406.839.1375
2020 Program Chair	Paul Inkenbrandt	paulinkenbrandt@utah.gov	801.537.3361
2020 Treasurer	Greg Gavin	greg@loughlinwater.com	801.538.4779
2020 Secretary	Elliot Jagniecki	ejagniecki@utah.gov	801.537.3370
2020 Past President	Peter Nielsen	peternielsen@utah.gov	801.537.3359

UGA Committees

Environmental Affairs	Craig Eaton	eaton@ihi-env.com	801.633.9396
Geologic Road Sign	Greg Gavin	greg@loughlinwater.com	801.541.6258
Historian	Paul Anderson	paul@pbageo.com	801.364.6613
Membership	Rick Ford	rford@weber.edu	801.626.6942
Outreach	Greg Nielsen	gnielsen@weber.edu	801.626.6394
Public Education	Zach Anderson	zanderson@utah.gov	801.537.3300
	Matt Affolter	gfl247@yahoo.com	
Publications	Paul Inkenbrandt	paulinkenbrandt@utah.gov	801.537.3361
Publicity	Paul Inkenbrandt	paulinkenbrandt@utah.gov	801.537.3361
Social/Recreation	Roger Bon	rogerbon@xmission.com	801.942.0533

AAPG House of Delegates

2020–2023 Term	David A. Wavrek	dwavrek@petroleumsystems.com	801.322.2915
----------------	-----------------	------------------------------	--------------

State Mapping Advisory Committee

UGA Representative	Bill Loughlin	bill@loughlinwater.com	435.649.4005
--------------------	---------------	------------------------	--------------

Earthquake Safety Committee

Chair	Grant Willis	gwillis@utah.gov	801.537.3355
-------	--------------	------------------	--------------

UGA Website — www.utahgeology.org

Webmaster	Paul Inkenbrandt	paulinkenbrandt@utah.gov	801.537.3361
-----------	------------------	--------------------------	--------------

UGA Newsletter

Newsletter Editor	Bill Lund	uga.newsletter@gmail.com	435.590.1338
-------------------	-----------	--------------------------	--------------

Become a member of the UGA to help support the work of the Association and receive notices for monthly meetings, annual field conferences, and new publications. Annual membership is \$20 and annual student membership is only \$5. Visit the UGA website at www.utahgeology.org for information and membership application.

The UGA board is elected annually by a voting process through UGA members. However, the UGA is a volunteer-driven organization, and we welcome your voluntary service. If you would like to participate please contact the current president or committee member corresponding with the area in which you would like to volunteer.



A Tale of Two Breccia Types in the Mississippian Leadville Limestone of Lisbon and Other Fields, Paradox Basin, Southeastern Utah

Thomas C. Chidsey, Jr.¹, David E. Eby², and Douglas A. Sprinkel³

¹Utah Geological Survey, Salt Lake City, UT 84114; tomchidsey@utah.gov

²Eby Petrography & Consulting, Inc., Denver, CO 80204; epceby@aol.com

³Utah Geological Survey, Salt Lake City, UT 84114; Azteca Geosolutions, Pleasant View, UT 84414; sprinkel@aztecageo.com

ABSTRACT

Two types of breccia are found in the Mississippian Leadville Limestone, Paradox Basin, southeastern Utah: (1) breccia associated with karstification and (2) breccia created by natural hydrofracturing, i.e., “autobreccia.” Breccia associated with sediment-filled cavities is relatively common throughout the upper one-third of the Leadville Limestone in Lisbon and other Paradox Basin oil and gas fields. These cavities and/or cracks are related to karstification of exposed Leadville during Late Mississippian time. Infilling of cavities by detrital carbonate and siliciclastic sediment occurred before deposition of the Pennsylvanian Molas Formation or Hermosa Group. Transported material consists of poorly sorted detrital quartz and feldspar grains, chert fragments, as well as clasts of carbonate and clay. Carbonate muds infilling karst cavities are very finely crystalline non-porous dolomites.

Post-burial brecciation, caused by natural hydrofracturing, is also quite common within Leadville reservoirs at Lisbon and other fields. Brecciation created an explosive-looking, pulverized rock, an “autobreccia” as opposed to a collapse breccia. Clasts within autobreccias remained in place or moved very little. Dolomite clasts are commonly surrounded by solution-enlarged fractures partially filled with coarse rhombic and late saddle dolomites. Areas between clasts exhibit good intercrystalline porosity and microporosity or are filled by dolomite cements. Intense pyrobitumen lining of pores was concurrent with, or took place shortly after, brecciation. The presence of zebra dolomites and zebra vugs attest to high temperatures associated with natural hydrofracturing. Rimmed microstructures or stair-step fractures are present, reflecting shear and explosive fluid expulsion from the buildup of pore pressure. Abundant pyrobitumen makes porous breccias and dolomites look like black “shales.” Post-burial breccias are associated with the best reservoir development at Lisbon field.

Outcrop analogs for both breccia types are present in the stratigraphically equivalent Mississippian section along the south flank of the Uinta Mountains in northeastern Utah. Based on field observations, a key component for autobrecciation is the presence of an underlying aquifer that serves as a conduit for hydrothermal fluids.

Large volumes of water throughput are required to produce brecciation and the amount, type, and generations of dolomite present at Lisbon field. We propose a model where convection cells bounded by basement-rooted faults transfer heat and fluids possibly from crystalline basement, Pennsylvanian evaporites, and Oligocene igneous complexes. Post-burial brecciation often results in the formation of large, diagenetic hydrocarbon traps.

Citation for this article.

Chidsey, T.C., Jr., Eby, D.E., and Sprinkel, D.A., 2020, A tale of two breccia types in the Mississippian Leadville Limestone of Lisbon and other fields, Paradox Basin, southeastern Utah: *Geology of the Intermountain West*, v. 7, p. 243–280, <https://doi.org/10.31711/giw.v7.pp243-280>.

© 2020 Utah Geological Association. All rights reserved.

For permission to use, copy, or distribute see the preceding page or the UGA website, www.utahgeology.org, for information. Email inquiries to GIW@utahgeology.org.

INTRODUCTION

The Mississippian Leadville Limestone is one of two major oil and gas plays in the Paradox Basin (figure 1), the other being the Pennsylvanian Paradox Formation (Chidsey and Eby, 2016; Chidsey and others, 2016). The Paradox Basin is within the west-central part of the Colorado Plateau physiographic province, southeastern Utah and southwestern Colorado. The Leadville is a shallow, open-marine carbonate shelf deposit having a variety of facies. Traps for hydrocarbons in the Leadville are fault and fault-related anticlines (figure 2), as is the case for Lisbon field (Morgan, 1993; Chidsey and Eby, 2016; Chidsey, in press). Hydrocarbon production and most drilling oil shows are found along the north-west-trending Paradox fold and fault belt in the northern part of the basin (figure 1).

Mississippian rocks in the Paradox Basin and other areas of the Colorado Plateau contain localized zones or pipes of breccia due to either collapse associated with paleokarstification or explosive natural hydrofracturing which created shattered-looking, pulverized rock, i.e., “autobreccia.” These characteristics are identified in several Leadville cores throughout the northern Paradox Basin. Breccia associated with sediment-filled collapsed cavities is relatively common in several areas and formed during periods of subaerial exposure. Autobreccia can be an irregular-shaped or cylindrical mass of brecciated rock that formed when hydrothermal solutions forced their way towards the surface through zones of weakness or fracture zones and naturally break up rocks in the process. The best examples of both breccia types are found in cores from Lisbon field, San Juan County, Utah (figure 1), which accounts for most Leadville oil and gas production in the Paradox Basin (~51.5 million barrels of oil [MMBO] produced as of January 1, 2020 [Utah Division of Oil, Gas and Mining, 2020]).

Porosity associated with karst breccias is often poor, whereas porosity in autobreccias and related dolomites can be very high in the Lisbon field area. However, saddle dolomite that formed as cement in autobreccia zones can reduce porosity. A key to identifying porous zones is the presence of abundant pyrobitumen, which makes porous breccias and dolomites appear like black “shales.”

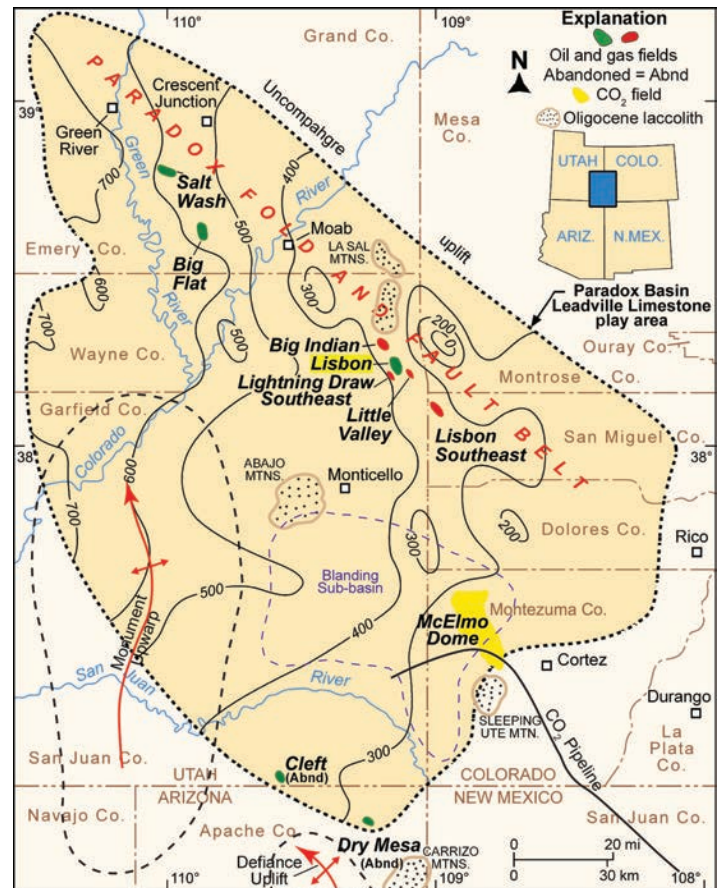


Figure 1. Regional setting of the Paradox Basin, showing fields (Lisbon highlighted) that produce oil and gas including carbon dioxide (CO₂) from the Mississippian Leadville Limestone, and thickness of the Leadville; contour interval is 100 feet (30 m). Modified from Parker and Roberts (1963). The Leadville Limestone Paradox Basin play area is colored dark tan. Modified from Morgan (1993).

The Mississippian strata along the south flank of the Uinta Mountains in northeastern Utah has similar characteristics to the Leadville Limestone. These rocks provide production-scale analogs of the facies and diagenetic characteristics, geometry, distribution, and nature of boundaries contributing to the overall heterogeneity of Leadville reservoirs. They also contain local zones of breccia due to either natural collapse or hydrofracturing and serve as a model for breccia formation in the Leadville Limestone.

The goal of this paper is to provide new information about two breccia types critical in understanding trapping mechanisms, reservoir quality and history, and

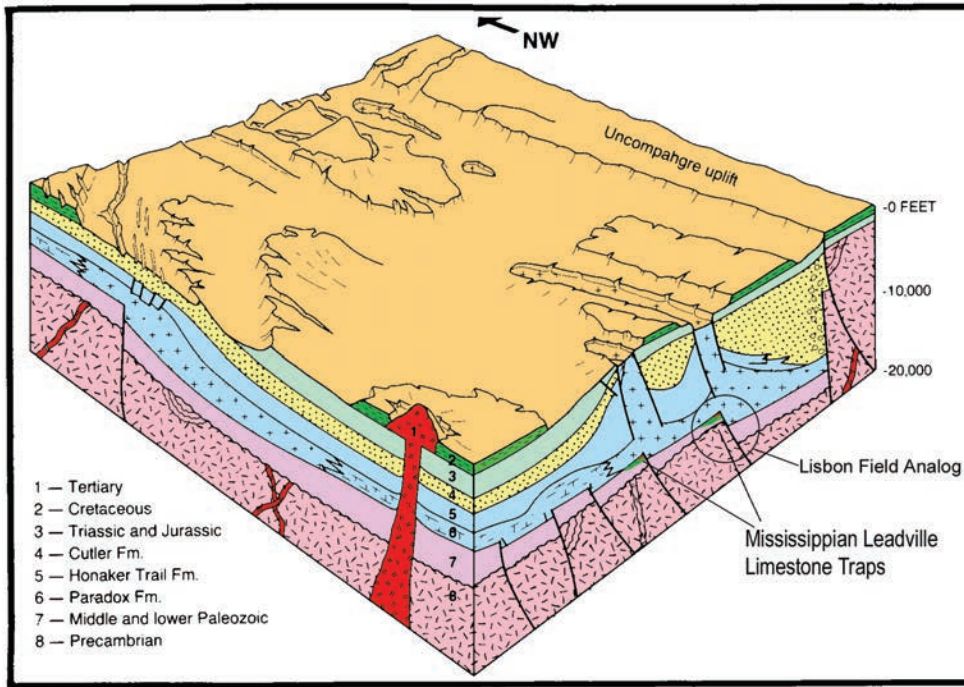


Figure 2. Schematic block diagram of the Paradox Basin displaying base-ment-involved structural trapping mechanisms for the Leadville Limestone fields. Modified from Petroleum Information (1984; original drawing by J.A. Fallin).

production in Leadville Limestone reservoirs. The understanding of breccia types can lead to identification of large, untapped diagenetic-type hydrocarbon traps in underexplored parts of the Paradox Basin and other analogous brecciated carbonate reservoirs.

General Characteristics of the Leadville Limestone

Depositional Environments

During the late Kinderhookian through early Meramecian, the Colorado Plateau was covered by a tropical, warm-water, shallow-shelf, variable energy epicontinental sea that covered a large part of the North American craton, with a shelf break into a deeper starved basin west of the Four Corners area (figure 3A). This platform was the site of extensive carbonate deposition implying arid, shallow marine conditions south of the paleoequator (Blakey and Ranney, 2008). Little sand or mud was transported into the shallow, clear water, providing favorable sites for growth of lime-secreting marine organisms, grains, and microbialites (Blakey and Ranney, 2008; Eby and others, 2014).

Mississippian marine fauna are corals, brachiopods, pelecypods, bryozoans, and crinoids; however, these fossil types are relatively rare in some areas. Other com-

mon biota include ostracods, benthic foraminifera, and gastropods. Microbial-dominated rocks are present, but uncommon. Depositional environments include mud-rich tidal flats; burrowed peloid mud in subtidal, intertidal, and supratidal settings; restricted marine; high-energy ooid shoals; middle shelf; storm-dominated, outer shelf open-marine, crinoid banks with mud-rich interbanks; and offshore low-energy, open-marine settings below wave base (figure 3B). Conditions in the interior of the Leadville carbonate platform were right for early marine reflux dolomitization derived from magnesium-bearing brines. Locally, mud-supported boundstone created buildups or mud mounds (Waulsortian facies), involving growth of “algae” (Wilson, 1975; Fouret, 1982, 1996; Ahr, 1989). Waulsortian buildups or mud mounds developed exclusively during the Mississippian in many parts of the world (Wilson, 1975).

During Late Mississippian (Chesterian) time, the entire carbonate platform in southeastern Utah and southwestern Colorado was subjected to subaerial exposure and erosion, resulting in the formation of a lateritic regolith (figure 4) (Welsh and Bissell, 1979). This regolith and associated carbonate dissolution (karstification) are important factors in Leadville reservoir potential.

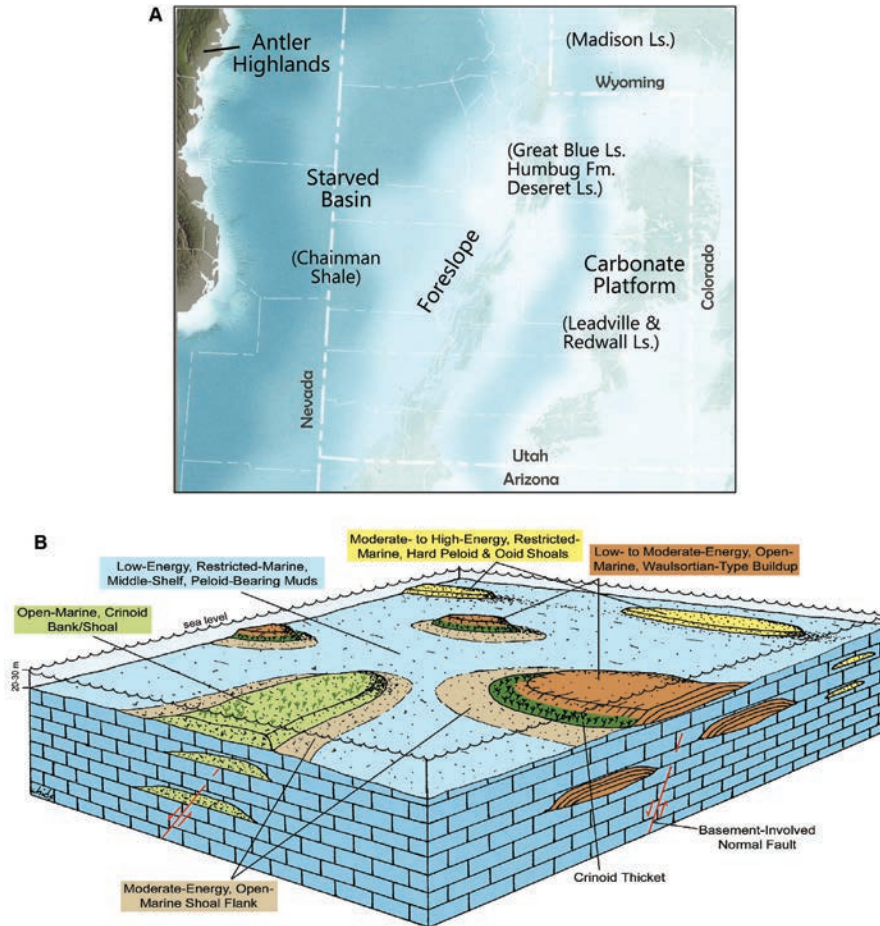


Figure 3. (A) Paleogeography of Utah during early Late Mississippian (early Meramecian) time when a warm shallow sea covered much of Utah. Modified from Blakey and Ranney (2008). (B) Block diagram for the Mississippian Leadville Limestone displaying major depositional facies during early Late Mississippian time, as determined from Lisbon field cores. From Chidsey and Eby (2016).

Lithology and Carbonate Fabrics

Mississippian formations are mostly light- to dark-gray, fine- to coarse-crystalline, cherty limestone. Dolomitic units are gray to tan, sucrosic to crystalline, and medium bedded with occasional silty partings. Both limestone and dolomite units are the main reservoir lithologies for the Leadville Limestone. Chert is typically light gray and forms lenses and nodules. The most common carbonate fabrics of the Leadville and other Mississippian formations include peloid, skeletal, and ooid grainstone, packstone, and wackestone; skeletal and intraclast rudstone and floatstone are also present. Cross-bedded grainstone fabrics of crinoid debris are

referred to as encrinites. Mudstones appear as microcrystalline and cryptocrystalline limestone and dolomite.

Stratigraphy

The Leadville Limestone is 300 to 600 feet (100–200 m) thick in the Paradox Basin (Hintze and Kowallis, 2009, and references therein) (figure 1). The Leadville Limestone is divided into two informal members (figure 5): (1) a dolomitic limestone lower member and (2) a limestone and dolomite upper member, separated by a regional disconformity within the Leadville. According to Baars (1966) this disconformity can be correlated

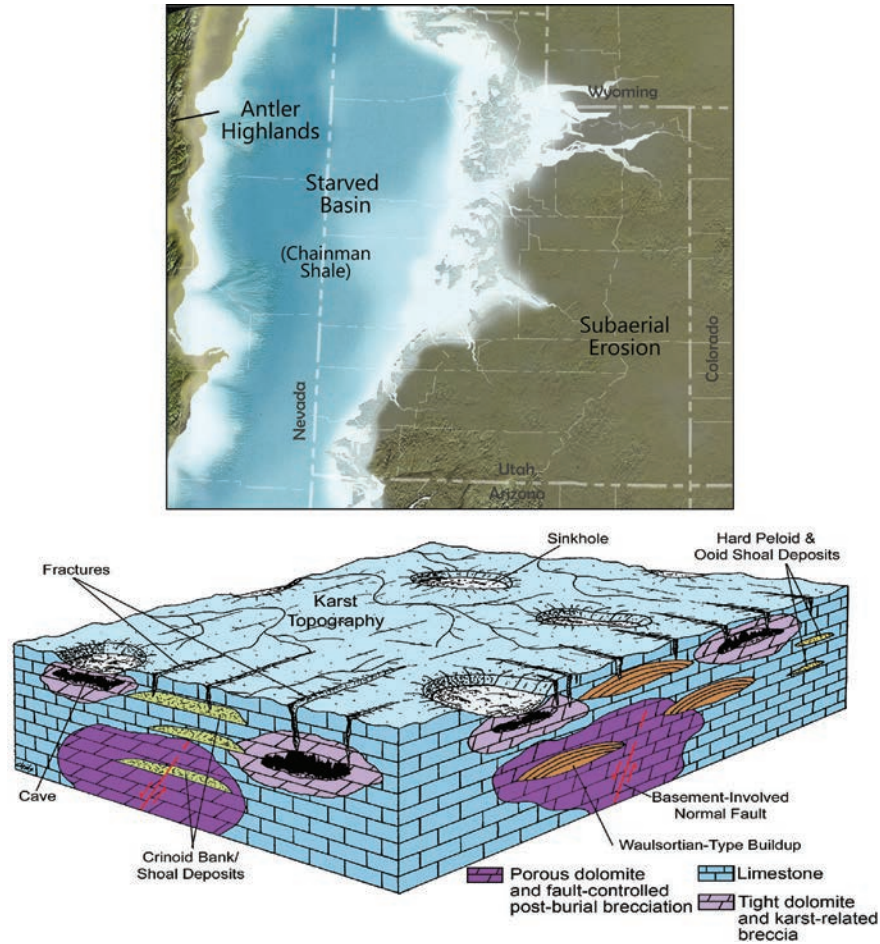


Figure 4. (A) Paleogeography during Late Mississippian (Chesterian) time when the entire carbonate platform in southeastern Utah and southwestern Colorado was subjected to subaerial erosion. Modified from Blakey and Ranney (2008). (B) Block diagram for the Mississippian Leadville Limestone displaying co-occurrence of karst-related breccias, cave sediments, and dolomites related to the exposed Leadville during Late Mississippian time with overprint of post-burial, fault-related breccias, fractures, and porous dolomites, as determined from cores in the Paradox Basin. After Chidsey and Eby (2016).

throughout the Paradox Basin. Brecciation and sediment-filled cavities, related to karstification of subaerially exposed Leadville in southwestern Colorado, are relatively common throughout the upper one-third of the formation (Evans and Reed, 2006, 2007). Average depth to the Leadville in Paradox Basin fields is 8760 feet (2920 m).

The Mississippian Leadville Limestone and overlying Pennsylvanian Molas Formation (where present) or Hermosa Group are separated by a major unconformity in southeastern Utah (figure 5). This same unconformity is found at the top of the stratigraphically equivalent Mississippian Redwall Limestone in the Grand Canyon (McKee, 1969), where subaerial exposure resulted in

development of karst topography with carbonate breccia-filled collapse features (paleo-sinkholes) and terra rosa (red earth cave fills) near the top of the formation. Similar features are recognized in Leadville cores. An unconformity separates the Leadville from the underlying Devonian Ouray Limestone (figure 5).

Lisbon Field, San Juan County, Utah

A wealth of core from Lisbon field is available at the Utah Core Research Center (UCRC) in Salt Lake City, Utah, as well as petrographic and other core-related data. Reservoir characteristics (Clark, 1978; Smith and Prather, 1981; Fouret, 1982, 1996; Chidsey and Eby,

Field Synopsis

Lisbon field is trapped within an elongate, asymmetric, northwest-trending anticline beneath the thick, salt-bearing Pennsylvanian Paradox Formation. The anticline has nearly 2000 feet (600 m) of structural closure and is bounded on the northeast flank by a major, basement-involved normal fault that has over 2500 feet (760 m) of displacement (Smith and Prather, 1981) (figures 6 and 7). Several minor, northeast-trending normal faults divide the Lisbon Leadville reservoir into compartments.

Producing units in Lisbon field contain crinoidal/skeletal dolograinstone, dolopackstone, and dolowackestone fabrics. Diagenesis includes fracturing, autobreciation, karst development, hydrothermal dolomitization, and bitumen plugging. Net reservoir thickness is 225 feet (69 m) over a 5120-acre (2100 ha) area (Clark, 1978; Smouse, 1993). Reservoir quality is improved by natural fracturing associated with the Paradox fold and fault belt. Porosity averages 6% in fracture-enhanced intercrystalline and moldic networks; permeability averages 22 millidarcies (mD). Reservoir drive is via an expanding gas cap and gravity drainage; original water saturation was 39% (Clark, 1978; Smouse, 1993). Bottom-hole temperature ranges from 133° to 189°F (56°–87°C).

Lisbon field was discovered in 1960 by the Pure Oil Company No. 1 NW Lisbon USA well (NE1/4NW1/4 section 10, T. 30 S., R. 24 E., Salt Lake Base Line and Meridian [SLBL&M]), San Juan County, Utah (figure 6), with an initial flowing potential of 179 barrels of oil per day (BOPD) and 4376 thousand cubic feet of gas per day (MCFGPD). The original reservoir field pressure was 2982 pounds per square inch (20,560 kPa) (Clark, 1978). Currently, 18 producing (or shut in) wells, 13 abandoned producers, 5 injection wells (4 gas injection wells and one water/gas injection well), and 4 dry holes are in the field. Cumulative production as of January 1, 2020, was 51,489,472 barrels of oil, 810.2 billion cubic feet of gas (cycled gas), and 50,600,821 barrels of water (Utah Division of Oil, Gas and Mining, 2020). Hydrocarbon gas, re-injected into the crest of the structure to control pressure decline, is now being produced; acid gas is still re-injected.

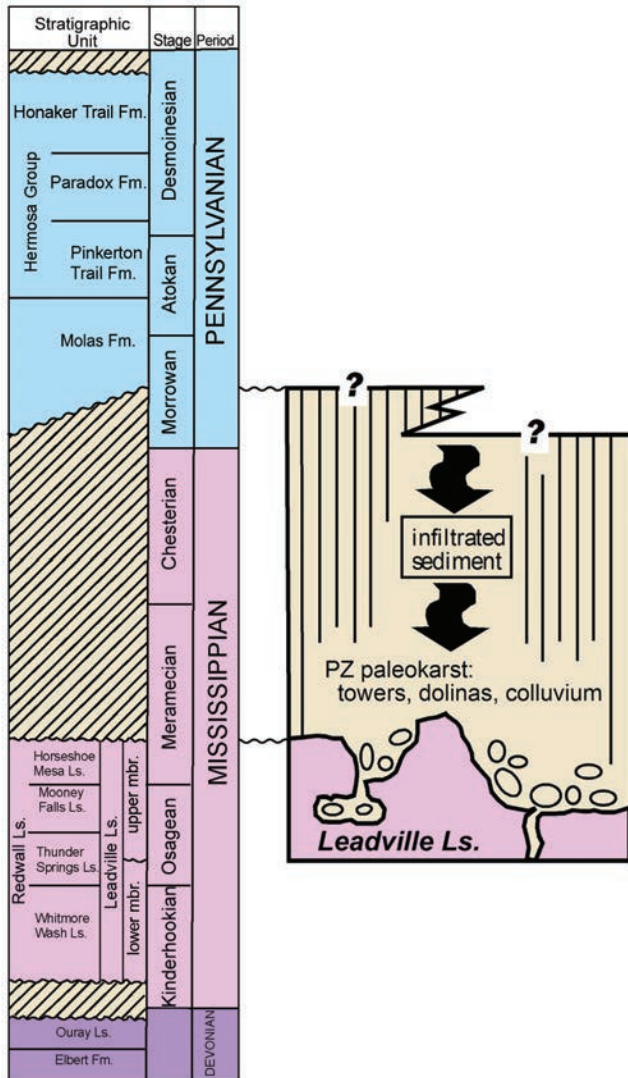


Figure 5. Devonian through Middle Pennsylvanian stratigraphic column for the Paradox Basin showing the major unconformity (defined by paleokarst features) between the Mississippian Leadville Limestone and the overlying Pennsylvanian Molas Formation. Note that the Leadville is divided into two informal members separated by an unconformity. Modified from Welsh and Bissell (1979) and Evans and Reed (2007).

2016), particularly brecciation from karstification and natural hydrofracturing, and Leadville facies can be applied regionally to other fields and exploration trends in the Paradox Basin. Therefore, we selected Lisbon as the major Leadville Limestone case-study field.

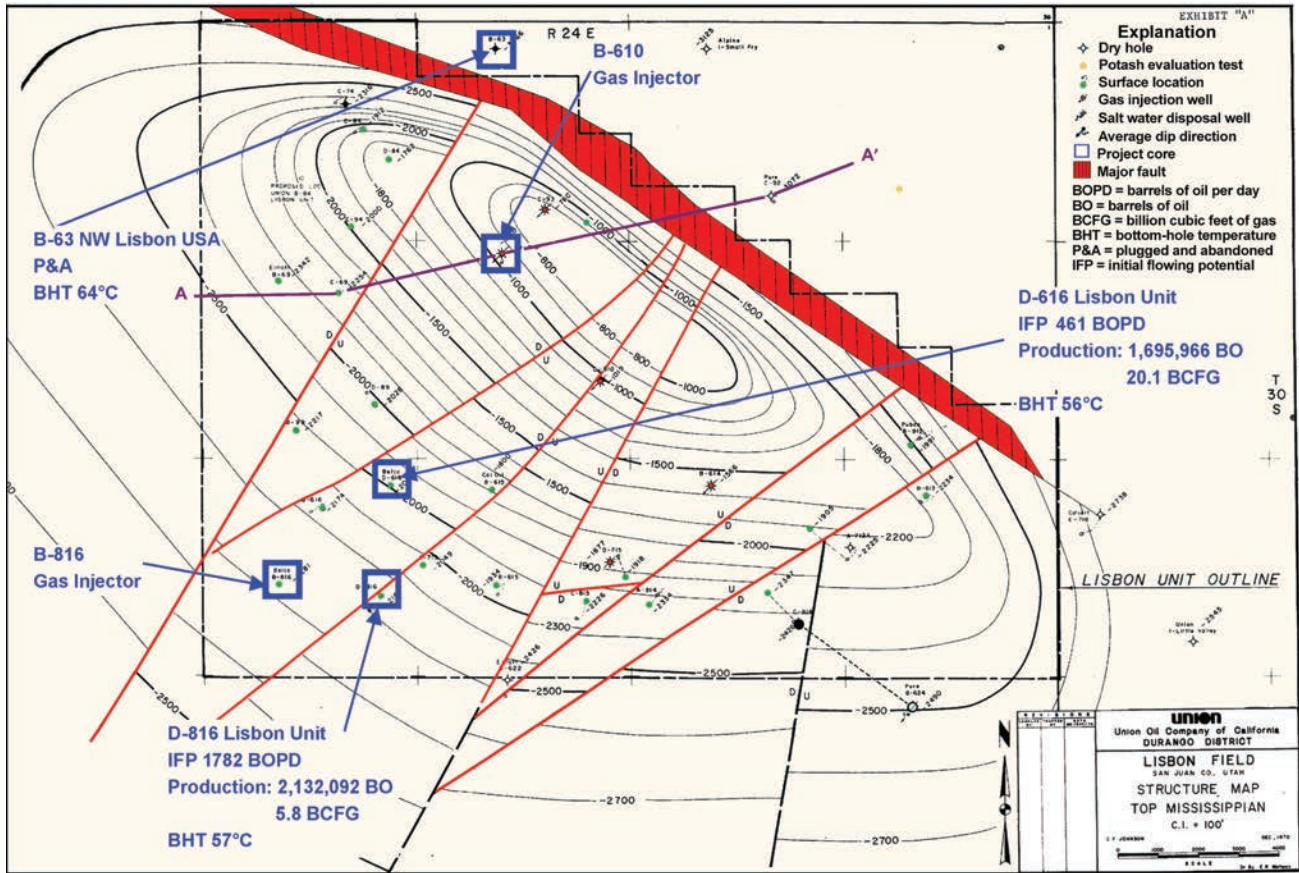


Figure 6. Top of structure of the Leadville Limestone, Lisbon field. Modified from C.F. Johnson, Union Oil Company of California files (1970) courtesy of Tom Brown, Inc. Cross section A–A' shown on figure 7. Also displayed are wells from which cores were described in this study.

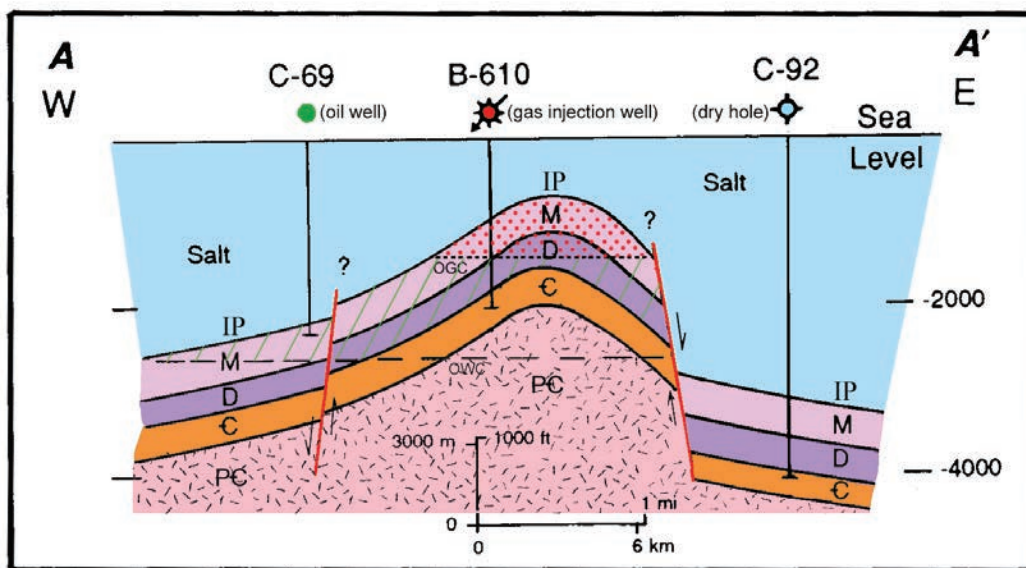


Figure 7. Schematic east-west structural cross section, Lisbon field. Line of section shown on figure 6. Note the juxtaposition of the Mississippian (M) section against the Pennsylvanian (IP) section, which includes evaporites (salt) and organic-rich shale. OGC = oil-gas contact, OWC = oil-water contact. Modified from Clark (1978).

Facies

Three primary depositional facies were identified in Leadville Limestone cores in the Lisbon case-study field: (1) open marine, (2) ooid and peloid shoals, and (3) middle shelf (figure 3B).

Open-marine lithofacies are represented by crinoidal banks or shoals and Waulsortian-type buildups (figure 3B). Crinoidal banks and shoals represent high-energy environments with well-circulated, normal-marine salinity water in a subtidal setting, although they can also be present in restricted marine, middle shelf settings. We estimate that water depths ranged from 5 to 45 feet (1.5–14 m). Waulsortian-type buildups were first described in Lisbon field by Fouret (1982) and are steep-sloped tabular, knoll, or sheet forms composed of several generations of mud deposited in a subtidal setting (Fouret, 1982, 1996; Lees and Miller, 1995) (figure 3B). Lime mud was precipitated by cyanobacteria (microbialites) (Lees and Miller, 1995). We estimate that water depths ranged from 60 to 90 feet (20–30 m).

Ooid and “hard” peloid shoals developed as a result of agitated, shallow-marine processes on the open-marine or bordering restricted-marine middle shelf (figure 3B). This lithofacies represents moderate to high energy, with moderately well-circulated water in a shoal setting. Sediment deposition and modification probably occurred in water depths that we estimate ranged from near sea level to 20 feet (6 m) below sea level within wave base.

Middle-shelf lithofacies covered extensive areas across the shallow platform and represent a low-energy, often restricted-marine environment (figure 3B). Mud and some sand were deposited in a low energy, subtidal (burrowed), inter-buildup/shoal setting. We estimate that water depths ranged from 60 to 90 feet (20–30 m).

Mississippian Outcrop Analogs in the Uinta Mountains

The Leadville Limestone is not exposed in southeastern Utah; however, equivalent Mississippian rocks outcrop along the flanks of the east-west-trending Uinta Mountains in northeastern Utah (figure 8). Uplift of the Uinta Mountains occurred during the Laramide

orogeny from latest Cretaceous time (Maastrichtian, about 70 Ma) through the Eocene (about 34 Ma). The Mississippian rock section along the southern flank of the Uinta Mountains is over 1600 feet (490 m) thick (Sprinkel, 2018) (figures 9 and 10). Mississippian outcrops along the western end of the Uinta Mountains consist of the Madison, Humbug, and Doughnut Formations (Bryant, 1990; figures 9 and 10). However, Bryant’s (1990) Madison includes the Fitchville Formation (Upper Devonian-Lower Mississippian [385–340 Ma]). In addition, the Madison includes a phosphatic shale interval identified by Sandberg and Gutschick (1980) and mapped by Sprinkel (2018) as the Delle Phosphatic Member of the Deseret Limestone. The Delle Phosphatic Member separates lower cliff-forming carbonate (Gardison Limestone) from upper cliff-forming carbonate (Deseret Limestone). Thus, the terms Gardison and Deseret Limestones are recommended for the western Uinta Mountains and are overlain by the Humbug and Doughnut Formations (figures 9 and 10). The Delle Phosphatic Member either pinches out or grades to mostly thin-bedded carbonate rocks in the eastern Uinta Mountains. Where the Delle is not recognized and the Gardison and Deseret cannot be easily separated, the term Madison Limestone is used (Sprinkel, 2006, 2007). For simplicity, the interval will be collectively referred to as the Mississippian section in this study. Contacts between the Mississippian formations in the Uinta Mountains are mostly conformable (Sadlick, 1955, 1957; Carey, 1973; Hintze and Kowallis, 2009).

Three sites were selected for detailed outcrop studies (figure 8): (1) South Fork Provo River, (2) Dry Fork Canyon, and (3) Crouse Reservoir/Diamond Mountain Plateau. Each study site has a unique set of depositional lithofacies and post-depositional breccia characteristics created by karstification and/or hydrofracturing in Mississippian strata that are identical or very similar to those observed in Leadville Limestone cores from Lisbon field in the Paradox Basin (figure 1), with samples collected for slabbing and thin section analysis. The South Fork Provo River study site is on the western end of the southern flank of the Uinta Mountains, Wasatch County (figure 8). The site is a series of roadcuts along the eastern side of State Highway 35, 11 miles (18 km) east of the town of Francis, and 25 miles (42 km) north-

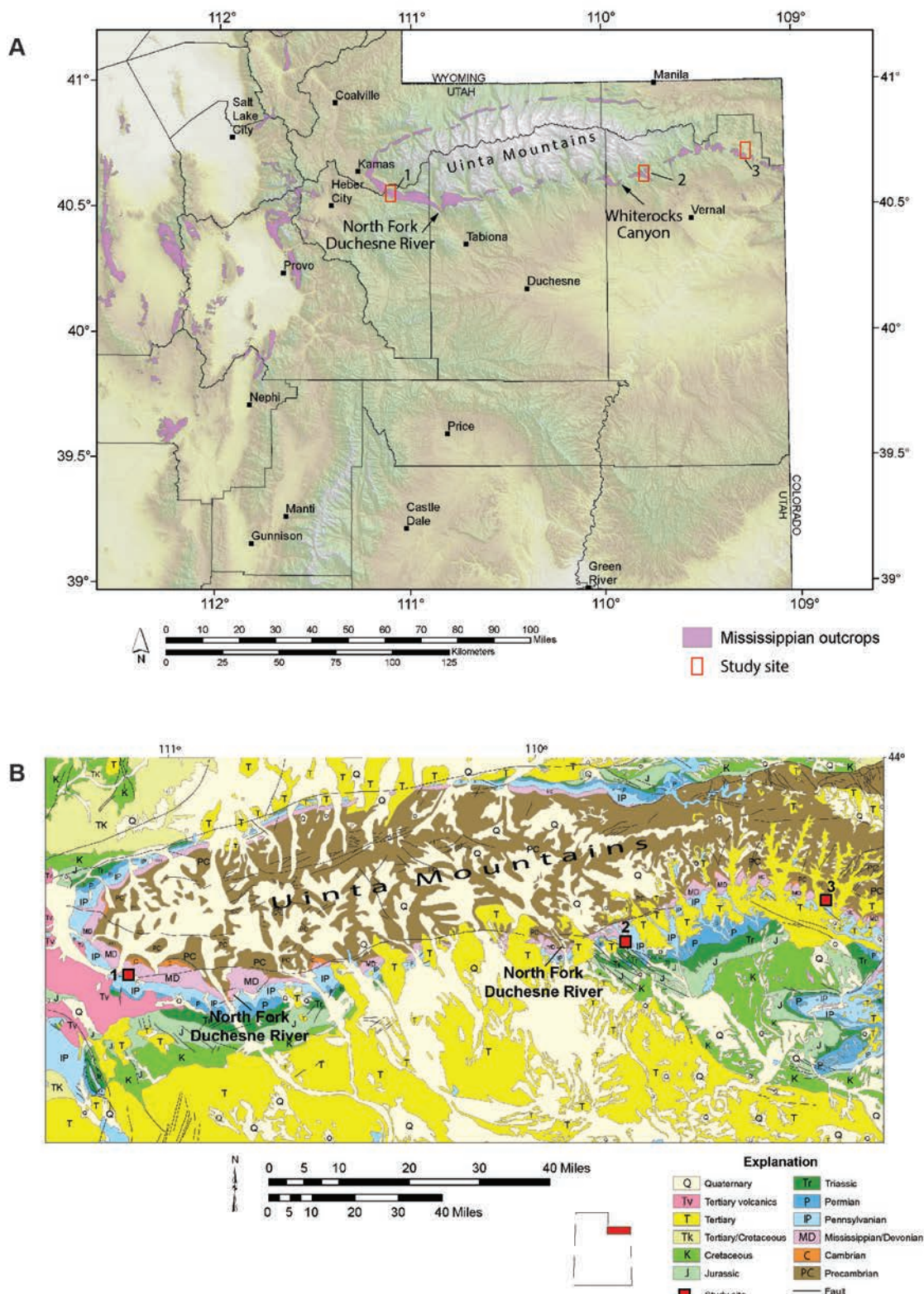


Figure 8. Mississippian outcrop reservoir analogs in Utah showing the location of the study sites. (A) Location of Mississippian rock outcrops in Utah equivalent to the Leadville Limestone. (B) Generalized geologic map of the Uinta Mountains, northeastern Utah. Modified from Hintze and others (2000).


Age	Formation		Thickness (ft)	Lithology
Permian	Oquirrh Group	Weber Sandstone	1700	
Pennsylvanian		Morgan Fm	200–325	
		Round Valley Ls	200–300	
Mississippian	Doughnut Fm		200–300	Solution cavities with breccia Delle Phosphatic Member
	Humbug Fm		360–410	
	Deseret Limestone		590–650	
	Gardison Limestone		250	
Devonian	Fitchville Fm		150	
Cambrian	Tintic Quartzite		0-395	
Precambrian	Uinta Mountain Group (part)	Red Pine Shale	0–1800	

Figure 9. Lithologic column of a part of the Paleozoic section along the western end of the southern flank of the Uinta Mountains. Modified from Hintze and Kowallis (2009) and Sprinkel (2018).


Age	Formation		Thickness (ft)	Lithology
Permian	Weber Sandstone		660-1320	
Pennsylvanian	Morgan Fm	Upper member	620-950	
		Lower mbr		
	Round Valley Ls		210-400	
Mississippian	Doughnut Shale		80-300	
	Humbug Fm		100-300	
	"Madison" Limestone		500-1000	
Cambrian	Lodore Formation		0-600	
Precambrian	Uinta Mountain Group		as much as 15,000	

Figure 10. Lithologic column of a part of the Paleozoic section along the eastern end of the southern flank of the Uinta Mountains. Modified from Hintze and Kowallis (2009).

west of the town of Hanna, Utah (figure 11). The Dry Fork Canyon study site is in the east-central part of the southern flank of the Uinta Mountains, Uintah County (figure 8), 20 miles (32 km) northwest of the town of Vernal, Utah. This site includes several noteworthy

outcrops along the Red Cloud Loop Road where it forks and turns up Brownie Canyon (figure 12). The Crouse Reservoir/Diamond Mountain Plateau study site is in the eastern part of the southern flank of the Uinta Mountains, Uintah County (figures 8 and 13), 29 miles (47 km) northeast of Vernal.

KARST BRECCIA, SEDIMENTS, AND OTHER CAVE DEPOSITS

Breccia created by karstification and cave sediments is found around the world where subaerial exposure of limestones is presently occurring or occurred during the geologic past. Excellent examples are found in Leadville Limestone and Mississippian rocks in the Uinta Mountains, northeastern Utah. Mississippian karst breccia and cave sediments resulted when much of the western North American craton, including eastern Utah, was subaerially exposed (figure 4).

Subsurface Leadville Limestone, Paradox Basin

A paleokarst lithofacies classification was developed for Leadville Limestone outcrops in Colorado by Evans

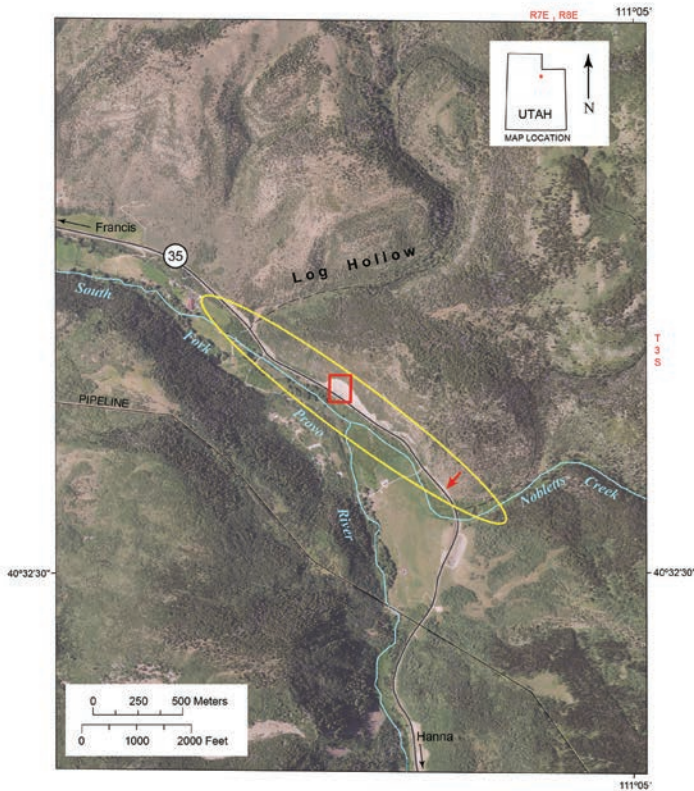


Figure 11. Google Earth image (© 2018 Google) showing the location of study site 1, South Fork of the Provo River and possible paleokarst features and the hydrothermal breccia pipe along the western end of the southern flank of the Uinta Mountains in Wasatch County, Utah. The Mississippian Desert Limestone outcrops are best exposed in roadcuts within the elongated yellow oval; the red arrow is the location of possible paleokarst features and the red square is the location of the breccia pipe.

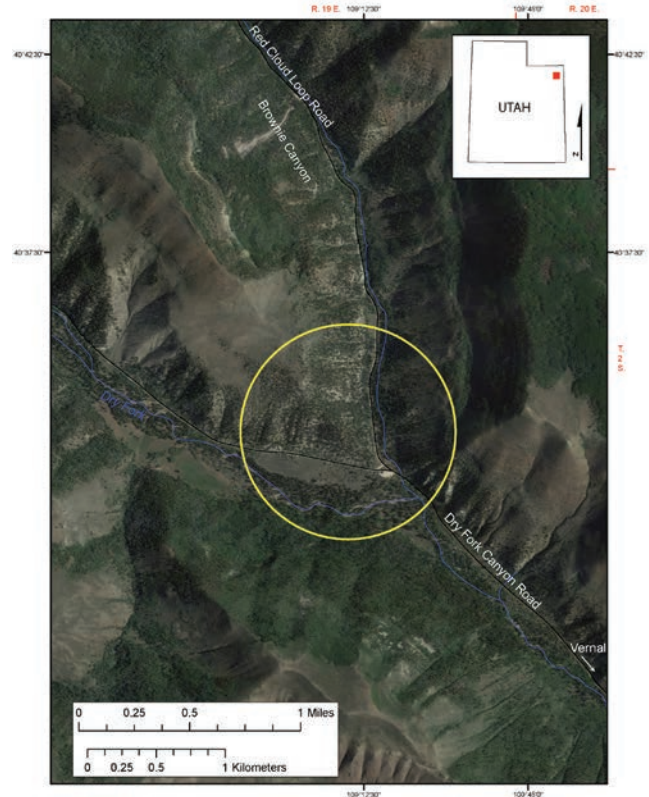


Figure 12. Google Earth image (© 2018 Google) showing the location of study site 2, Dry Fork Canyon (yellow circle).

and Reed (2006, 2007) (table 1). We characterized paleokarst lithofacies, as well as post-burial autobreccia, from regional and Lisbon field wells (figure 14). Five cave sediment lithofacies were recognized in three cores based on the Evans and Reed (2006, 2007) classification: (1) speleothem, (2) breccia, (3) fissure-fill sediments, (4) conglomerate, and (5) fine-grained sediment.

Speleothem

A speleothem is defined as any natural secondary mineral deposit formed in a cave by water movement. Speleothems take on a variety of forms depending on whether groundwater drips, seeps, condenses, flows, or ponds (Hill and Forti, 1997). Most speleothems are

calcareous and composed of calcite or aragonite. In the case of the Leadville Limestone, they originated in situ essentially where they are found (autochthonous) within vadose paleocave passages and consist of dripstone, flowstone, cave pearls (a small spherical speleothem with concentric layers around a nucleus), a variety of cave crystals, and many other types (Evans and Reed, 2006, 2007). Caves are commonly decorated with dripstone in the form of stalactites, stalagmites, and columns. Flowstone is a sheet-like deposit on the cave floors and walls and can also form cave drapery (thin, wavy sheets of calcite or aragonite that hang downward from the roof of the cave) or rimstone dams that appear like stairs and build up in pools of water.

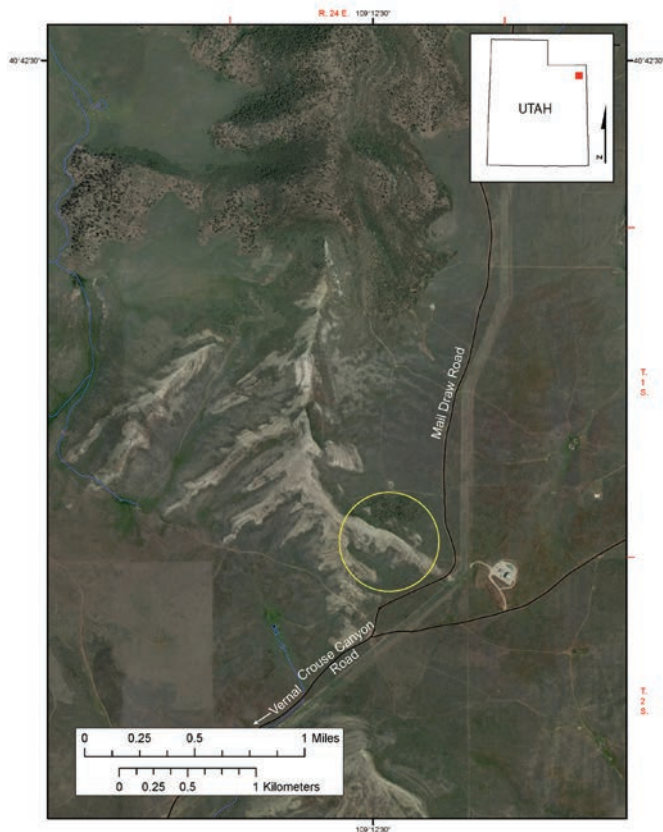


Figure 13. Google Earth image (© 2018 Google) showing the location of study site 3, Crouse Reservoir/Diamond Mountain Plateau (key brecciated outcrop indicated with yellow circle).

A speleothem was identified in core from the Big Flat No. 2 well (figures 14 and 15). The speleothem, most likely sheet-like flowstone of calcite, caps a karst breccia. No other speleothems were identified in the cores examined.

Breccia

Breccia, formed via karstification, is common in many cores examined in the study. The breccia consists of a chaotic mix of various clast sizes infiltrated with a siliciclastic matrix. Cave breccia in the Leadville Limestone developed in the vadose zone and originated near or not too far from where they are found (parautochthonous) under paleosinkholes (also called paleodolines) or from the creation of breakout domes (large rooms formed when the cave ceiling collapsed) (Loucks, 1999; Evans and Reed, 2006, 2007).

An excellent example of cave breccia is shown in core from the Big Flat No. 2 well (figures 14 and 16). The breccia consists of angular chaotic clasts ranging from pebbles to boulders(?) in a greenish-gray siliciclastic matrix.

Fissure-Fill Sediments

Fissure-fill sediments, often referred to as geopetal, represent infilling of open, solution-enlarged fissures, fractures, or joints (grikes) (Evans and Reed, 2006, 2007). Leadville Limestone fissure-fill geopetal sediment developed in the vadose zone and generally originated in a place other than where they are found (allochthonous). They may be horizontally or vertically laminated depending on whether their formation was due to successive events or reopening of closed fissures, respectively (Evans and Reed, 2006, 2007). Other fissure fills can be massive (cave fill).

Both laminated and massive fissure-fill sediments were identified in core from the Big Flat No. 2 and No. 3 wells, respectively, and in Lisbon field (figure 14). Vertically laminated fissure-fill sediments (geopetal) infiltrated into linear and curvilinear, dissolution-enlarged fractures and dissolution cavities (vugs) (figure 17). Dissolution features are often funnel-shaped, especially with massive-fissure fills in large, dissolution cavities (figure 18). Massive fissure-fill sediment alternates between clay and loessite (lithified paleoloess) deposits. Fissure-fill sediments in these cores likely originated from the overlying Pennsylvanian Molas Formation above the regional unconformity (figure 5).

Conglomerate

Cave conglomerates are massive to poorly stratified (Miall, 1978; Evans and Reed, 2006, 2007). Sorting is poor, clasts are subrounded to subangular, and conglomerate is clast supported. Leadville Limestone cave conglomerates developed in both vadose and phreatic zones and, like the fissure-fill sediments (geopetal), are allochthonous.

Conglomerates were identified in core from the Big Flat No. 2 well (figures 14 and 19). Unlike solution rounded limestone and chert described by Evans and Reed (2006, 2007) in table 1, poorly stratified conglom-

Table 1. Paleokarst lithofacies classification developed for Leadville Limestone exposures in Colorado by Evans and Reed (2006, 2007).

Lithofacies	Description	Interpretation	Origin
Speleothem (S) Sf flowstone Sd: dripstone Sc: cave pearls	Carbonate buildups as mounds or sheets of calcite spar or as radially banded calcite spar (cave pearls), interbedded with red siliciclastics.	In situ chemical precipitates in vadose paleocave passages.	Autochthonous (Vadose Zone)
Breccia (B) Br: chaotic, mosaic, or crackle breccia	Clast-supported, limestone-chert boulder-pebble breccia, with infiltrated red siliciclastic matrix.	Cave collapse breccia formed due to roof collapse in breakout domes or paleodolines.	Paraautochthonous (Vadose Zone)
Fissure-fill Sediments (J) Jl: laminated fissure-fills Jm: massive fissure-fills	Funnel-shaped dissolution features infilled by infiltrated red loessite from the overlying Molas Formation mixed with locally derived gravel-sized, angular limestone or chert clasts.	Gravity infilling of open fissures or joints (grikes). Horizontal lamination represents successive infilling events. Vertical lamination represents the re-opening of closed fissures due to shifting of underlying blocks.	Allochthonous (Vadose Zone)
Diamict (D) Dmm: massive diamict Dms: stratified diamict	Pebble-cobble diamicts with siltstone-rich matrix. Some vertical clast orientations.	Debris (siltstone-rich, subaqueous debris-flow deposits).	Allochthonous (Vadose and Phreatic Zones)
Conglomerate (G) Gm: massive to poorly stratified conglomerate	Clast supported, imbricated conglomerate consisting of solution rounded limestone and chert clasts with siltstone intraclasts.	Coarse-grained fluvial cave sediment. Represents bedload transport of locally derived clasts through phreatic tubes.	Allochthonous (Vadose and Phreatic Zones)
Sandstone (SN) SNr: ripple-laminated and climbing-ripple laminated sandstone	Fine-grained, silty sandstone with climbing-ripple lamination.	Fine-grained fluvial cave sediment. Represents rapid sedimentation rates.	Allochthonous (Vadose and Phreatic Zones)
Siltstone (SS) SSm: massive siltstone	Massive, sandy siltstone that can show primary current lineation.	Fine-grained fluvial cave sediment. The abundant siltstone is a legacy of the loessite source material. Primary current lineation indicates upper flow regime conditions.	Allochthonous (Vadose and Phreatic Zones)
Fine-grained Sediments (F) Fl: laminated siltstone-mudstone rhythmite Fm: massive silty mudstone Fed: claystone drape with mudcracks	Argillaceous quartz siltstone, siltstone-claystone rhythmites, and mudstone drapes, often with mudcracked upper surfaces.	Fine-grained fluvial cave sediment. The abundant siltstone is a legacy of the loessite source material. The rhythmites are siltstones with thin mudstone partings.	Allochthonous (Vadose and Phreatic Zones)

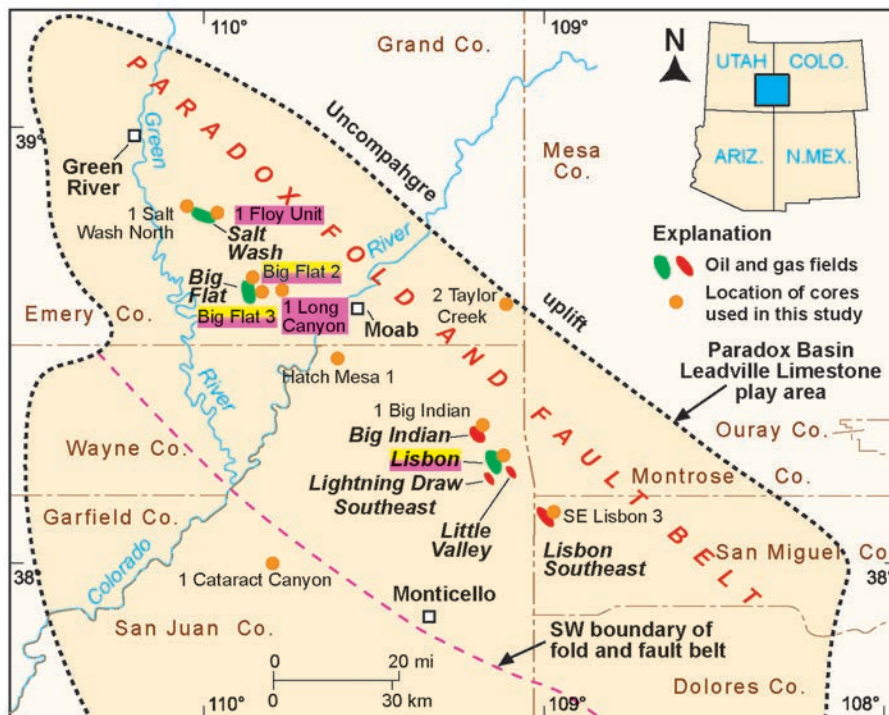


Figure 14. Location of wells in the Paradox fold and fault belt with cores used for examples of (1) karst breccia and cave sediment lithofacies (highlighted in yellow), and (2) post-burial breccia, pyrobitumen, dolomitization, and porosity (highlighted in pink).

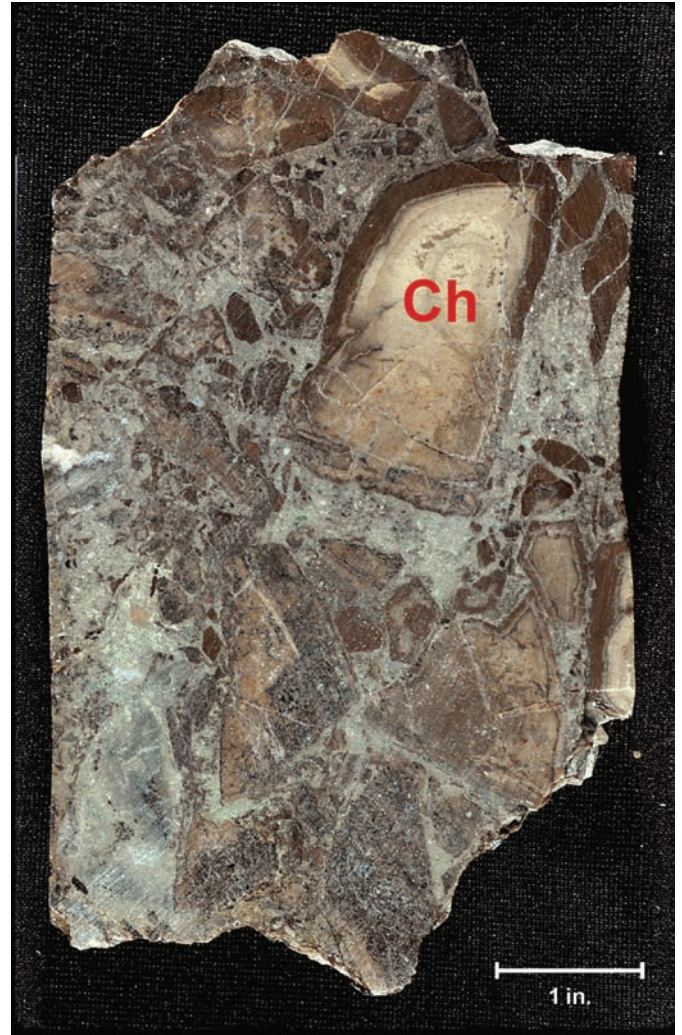


Figure 15. Karst breccia with speleothems (red arrows) capping massive to poorly stratified conglomerate consisting of pink feldspathic sandstone and granitoid clasts between Leadville Limestone country rock. Big Flat No. 2 well (section 11, T. 26 S., R. 19 E., SLBL&M, Grand County, Utah, figure 14), slabbed core from 7729 to 7730 feet (2355.8–2356.1 m).

Figure 16. Typical cave breccia infiltrated with a siliciclastic matrix. Note the clast-supported early chert (Ch). Big Flat No. 2 well (figure 14), slabbed core from 7744 feet (2360 m).

erate in the Big Flat No. 2 core consists of granitic clasts in a matrix of pink feldspathic sand. This coarse-grained cave sediment fill may have been associated with fluvial sedimentation within the Leadville cave system.

Fine-Grained Sediment

Fine-grained sediment in caves consists of quartz siltstone, silt-rich mudstone, siltstone-mudstone rhythmites, or mudstone drapes (Miall, 1978; Evans and Reed, 2006, 2007). In the Leadville Limestone, fine-

grained sediments were deposited in both vadose and phreatic zones, are allochthonous, and laminated or massive. Source of Leadville fine-grained sediments in southwestern Colorado is loess where the Mississippian paleokarst served as a “dust trap” for identical deposits in the overlying Pennsylvanian Molas Formation (figure 5); the provenance for the loess is unknown because the silt is composed almost entirely of quartz and there are no paleocurrent features (Evans and Reed, 2006, 2007). Fine-grained sediment may also represent fluvial cave

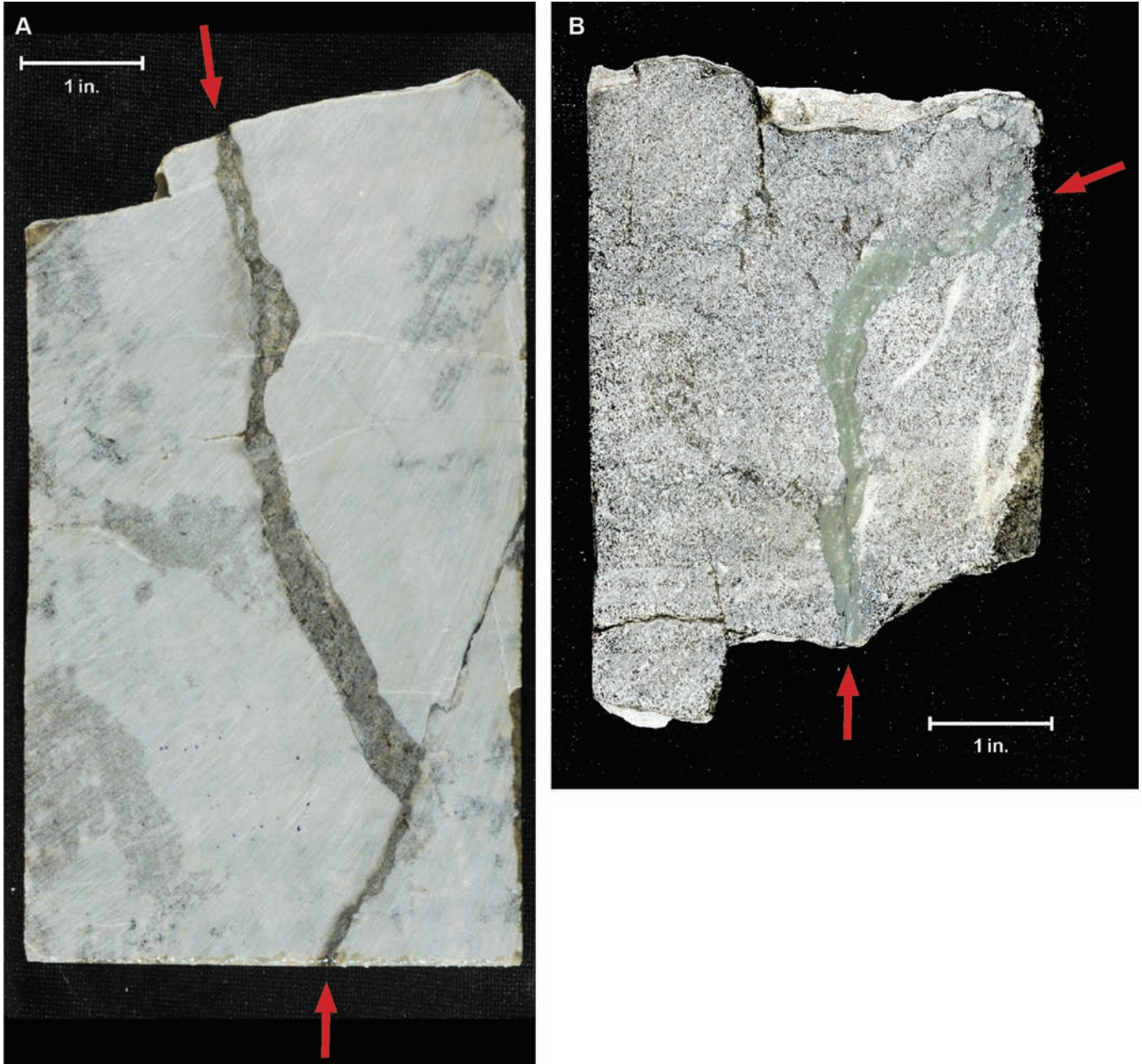


Figure 17. Vertically laminated fissure-fill sediments (between red arrows) infiltrated into (A) a linear dissolution-enlarged fracture or joint (grike) developed within a well-bedded peloidal/skeletal wackestone, and (B) a curvilinear to funnel-shaped dissolution cavity developed within a well-bedded oolitic/peloidal grainstone. Big Flat No. 2 well (figure 14), slabbed core from 7724.5 feet (2354.4 m) (A) and 7631 feet (2326 m) (B).

sediment (Evans and Reed, 2006, 2007).

Both laminated and massive fine-grained sediment were identified in cores from the Big Flat No. 2 and No. 3 wells, respectively (figures 14 and 20). Fine-grained sediment in these cores is silt-rich mudstone. Laminated fine-grained sediment infiltrated between solu-

tion-modified clasts (figure 20A). Massive bedded strata infiltrated into a dissolution cavity (vug) (figure 20B).

Cave-Fill Sediments in Lisbon Field

Fissure-fill sediments and sediment-filled cavities are common throughout the upper one-third of the



Figure 18. Massive fissure-fill sediments consisting of clay and loessite infiltrated into a large dissolution cavity developed within a well-bedded peloidal/oolitic grainstone. Big Flat No. 3 well (section 23, T. 26 S., R. 19 E., SLBL&M, Grand County, Utah, figure 14), slabbed core from 7677 feet (2340 m).



Figure 19. Cave breccia consisting of large, poorly sorted, white angular clasts of fractured limestone (or dolomite) surrounded by a yellowish altered matrix of feldspathic and granitic conglomerate and sandstone. Note also the greenish clay and black bitumen. Big Flat No. 2 well (figure 14), slabbed core from 7630.5 feet (2325.8 m).

Leadville Limestone in Lisbon field (figures 14 and 21). Contacts between transported material and country rock can be sharp, irregular, and corroded with small associated mud-filled fractures (figures 21A and 21B). Transported material consists of poorly sorted detrital quartz grains (silt size), chert fragments, carbonate clasts, clay (figure 21C), and occasional clasts of mud balls (desiccated and cracked). Infilling sediment displays crude lamination.

Carbonate mud infiltration of karst cavities is dolo-

mitized (later diagenetic process), consists of very fine crystals, and is non-porous (figures 21 and 22); porosities are less than 2% and permeability is about 11 mD. Typically, the surrounding limestone matrix is also non-porous.

Other karst features observed in Leadville thin sections include (1) the presence of “root hairs,” i.e., thin, sinuous cracks filled with dolomitized mud, and (2) clasts with a coating of clay. Both of these features may be indicative of a soil zone.

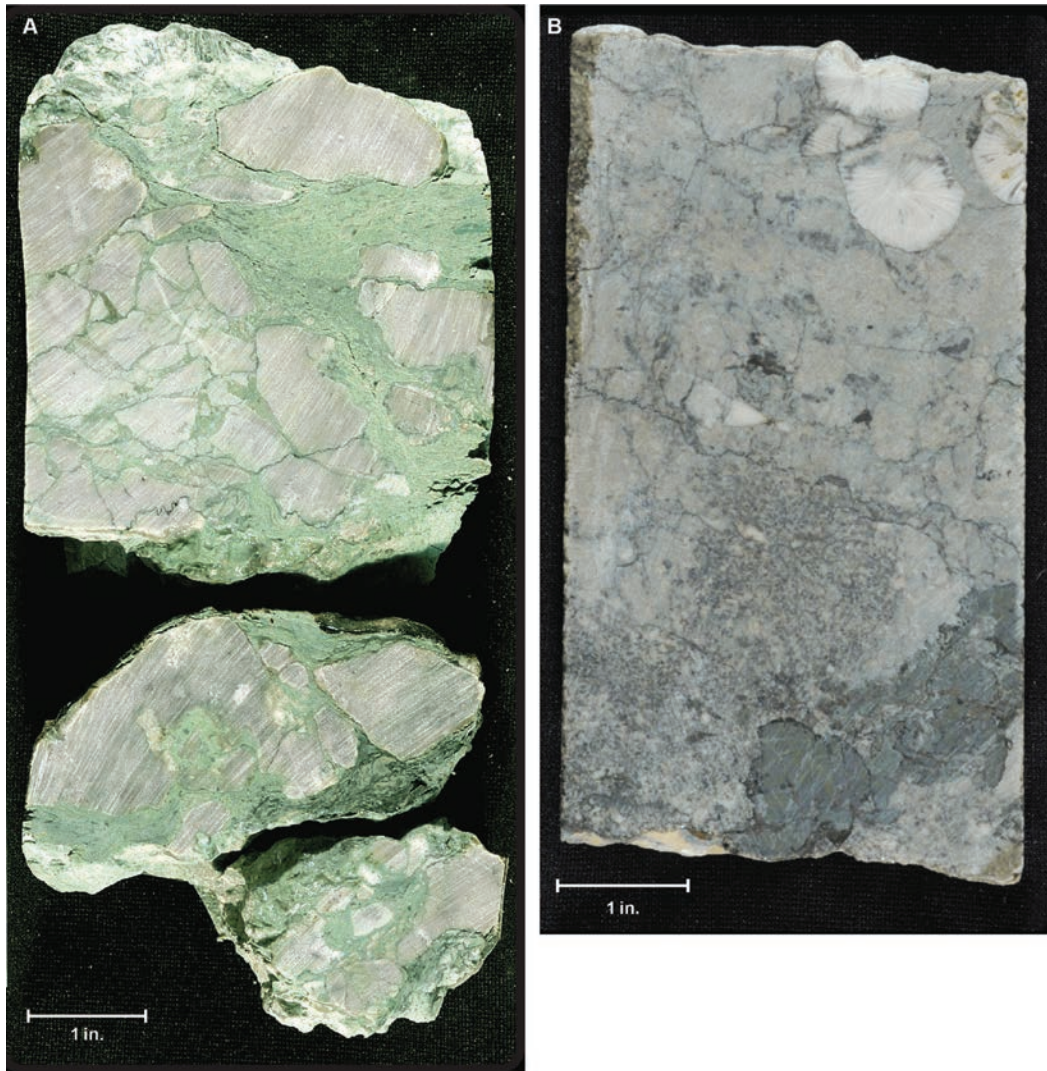


Figure 20. Fine-grained sediment. (A) Laminated silty green mudstone infiltrated between solution-modified clasts of Leadville peloidal mudstone. Big Flat No. 2 well (figure 14), slabbed core from 7737 to 7738 feet (2358.2–2358.5 m). (B) Massive silty mudstone infiltrated into a dissolution cavity developed within a crinoidal/skeletal grainstone (with rugose corals). Big Flat No. 3 well (figure 14), slabbed core from 7723.5 feet (2354.1 m).

Karstification in Uinta Mountain Mississippian Outcrops

Study Site 1 – South Fork Provo River

Study site 1, South Fork Provo River, and the surrounding area was mapped by Eskelsen (1953), McDougald (1953), and Bryant (1990). Sprinkel (2018) mapped an adjacent area along the southern flank of the Uinta Mountains and western Uinta Basin. The primary outcrop containing breccias is in the Deseret Limestone (Osagean through middle Meramecian). The contact with the overlying Humbug Formation is difficult to recognize due to the poor nature of the outcrops and extensive slope cover. Eskelsen (1953) and McDougald (1953) mapped the area as Deseret-Humbug undiffer-

entiated. Bryant (1990) mapped Fitchville, Gardison, and Deseret together in the area of the breccias at study site 1 with Humbug mapped separately. Elsewhere, Bryant (1990) mapped each formation as separate units. Although Bryant (1990) lumped Fitchville, Gardison, and Deseret together at study site 1, our examination of these outcrops determined that rocks containing breccias are Deseret.

The Deseret Limestone at study site 1 is a dark- to light-gray limestone consisting of skeletal grainstone to packstone (figure 23) representing a high-energy, open-marine environment. In Deseret outcrops at study site 1, possible paleokarst features have similar characteristics found in Leadville cores (as well as outcrops of the equivalent Mississippian Redwall Limestone in the Grand Canyon). Stratiform polymictic brecciation

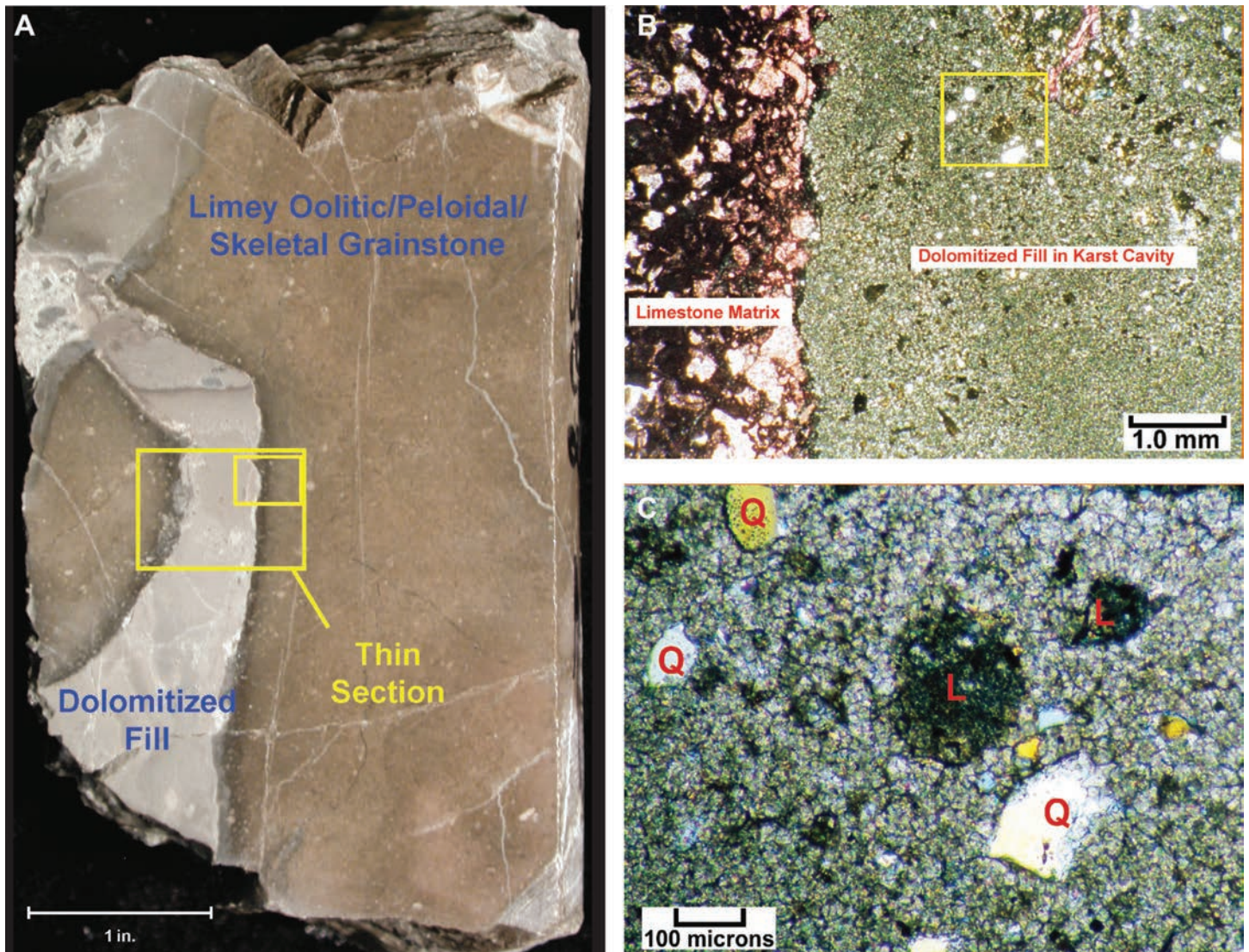


Figure 21. Karst-related processes at Lisbon field. (A) Core slab of a limey, oolitic, peloidal/skeletal grainstone (brown) and dolomitized silty carbonate sediment (light gray) that filled a solution-enlarged cavity or fissure. The smaller yellow box indicates the approximate position of the thin section photomicrograph shown on B. (B) Low-magnification photomicrograph (plane light) showing the contact between the non-porous limestone matrix (stained red for calcite) and the equally non-porous dolomitized and siliciclastic karst cavity filling. The yellow box indicates the approximate position of the close-up photomicrograph shown on C. (C) Higher magnification photomicrograph (cross-polarized light) of white detrital quartz grains (Q) and small dark gray carbonate clasts (L) within the non-porous, dolomitized mud filling the karst cavity. Lisbon No. D-616 well (figure 6), 8308 to 8309 feet (2532.3–2532.6 m), porosity = 1.2%, permeability = 11.1 mD.

(collapse) is extensive (figures 24A and 24B), but without calcite veins, dolomitization, and explosive characteristic of a breccia pipe. Red staining at the top of the Deseret Limestone, mapped as the Madison Limestone by Bryant (1990), is possible terra rosa (red earth) weathering (i.e., reddish-colored clay-rich layer containing hematite that ranges in thickness from a few

inches to several feet and can be found coating limestone in ancient and modern karst areas), but could be coming from the overlying Humbug Formation (figure 24C). Karstification and formation of collapse breccias may have begun shortly after deposition of the Deseret, which would argue for an unconformity between the Deseret and Humbug; however, this has not been

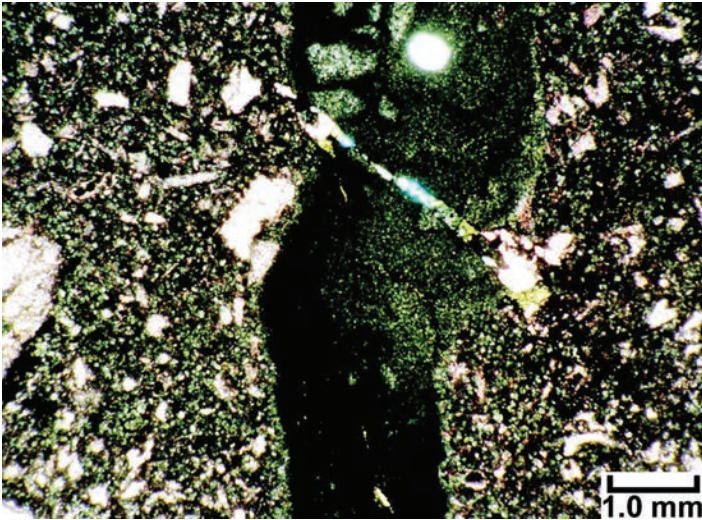


Figure 22. Photomicrograph of another example of a non-porous, dolomitized sediment filling of a karst cavity in this low-magnification view (plane light and stained red for calcite). In addition, there is no visible porosity within the partially dolomitized crinoidal grainstone matrix. Lisbon No. D-616 well (figure 6), 8356 to 8357 feet (2546.9–2547.2 m).



Figure 23. Skeletal (crinoid and rugose coral) grainstone and packstone in the Deseret Limestone at study site 1 (within the yellow oval on figure 11).

identified elsewhere. Several sinkholes are mapped in undivided Deseret and Humbug outcrops, as well as in the Gardison Limestone and Weber Sandstone (Pennsylvanian-Permian), in the area by Eskelsen (1953). Karst-related features likely postdate the Mississippian, beginning as early as late Eocene to Oligocene (Godfrey, 1985; Spangler, 2005). Mayo and others (2010) suggested the cave system formed relatively recently (Pleistocene).

Study Site 2 – Dry Fork Canyon

The Dry Fork Canyon stratigraphic section demonstrates heterogeneity as well as cyclicity (two shoaling upward cycles) of Madison Limestone depositional environments within a 40-foot-thick (12 m) outcrop (figure 25). The base of the section is oolitic/hard pellet grainstone with well-defined, planar to low-angle cross-stratification representing a beach/foreshore depositional environment. The next unit is a wavy to bioturbated, peloidal/skeletal packstone to grainstone with hard pellets, benthic forams, and other microfossils indicative of a stable, shallow, subtidal bay depositional environment. The section coarsens up to oolitic/hard pellet grainstone with small- to medium-scale cross-stratifi-

cation representing an ooid shoal. Tidal-flat mud and deeper, subtidal, burrowed, pellet mud overlies the ooid shoal consisting of soft pellet mudstone with crinkly continuous cryptalgal (microbial) laminates and skeletal microfossils (ostracods and benthic forams). These sediments are overlain by thin-bedded to bioturbated, peloidal/skeletal packstone to grainstone with endothyrid forams and other microfossils indicating return to a stable, shallow, subtidal bay. The cycle continues to coarsen upward with low- to medium-angle cross-stratified oolitic grainstone of an ooid shoal. The top of the section is mudstone with continuous cryptalgal laminates (microbial), pellets, possible desiccation cracks and rip-up clasts, and no fossils, all features indicative of a peritidal tidal-flat mud. The Madison at this site is predominately dolomite.

Several post-depositional features can be found at study site 2. A megabreccia is exposed at the western end of the Madison outcrop where the section was described (figure 26A). This breccia is a paleokarst collapse where limestone and dolomite clasts are set in a non-porous mud-rich matrix. In thin section (figure 26B), this breccia appears similar to collapse breccia seen in core from Lisbon field (compare to figure 21).



Country rock is cross-bedded, oolitic dolograins (oid shoal) capped by low-angle, stratified dolograins (foreshore) (figure 26A).

POST-BURIAL BRECCIA

Post-burial brecciation can be formed by high-temperature hydrofracturing, creating an explosive looking, pulverized rock referred to as an “autobreccia” as opposed to a collapse breccia. Breccia clasts within an autobreccia remain in place or moved very little. Similar to brecciation associated with collapse due to karstification, excellent examples of autobreccia are found in the Leadville Limestone and Mississippian rocks of the Uinta Mountains, northeastern Utah.

In addition to autobrecciation, late dolomitization, saddle dolomite, and dolomite cement precipitation may have occurred at progressively higher temperatures, i.e., hydrothermal dolomite. Hydrothermal events can improve reservoir quality by increasing porosity through dissolution, dolomitization, development of microporosity, and natural fracturing (forming breccia) and kept open with various minerals (Smith, 2004, 2006; Davies and Smith, 2006; Smith and Davies, 2006). Hydrothermal dolomite precipitates under temperature and pressure conditions greater than the ambient temperature and pressure of the host limestone (Davies, 2004; Davies and Smith, 2006; Smith, 2006; Smith and Davies, 2006). The result can be formation of large, diagenetic-type hydrocarbon traps.



Subsurface Leadville Limestone, Paradox Basin

Cores from Leadville Limestone wells in the Paradox fold and fault belt (figure 14) and Lisbon field (figure 6) reveal that autobrecciation due to hydrofracturing was common. Associated with autobreccia are pyrobitumen linings, saddle and zebra dolomite, rimmed microstructures or stair-step fractures, and porosity development or reduction.

Autobreccia, Pyrobitumen, and Porosity

Autobrecciation is characterized by massive fracturing and stylolites, which control post-burial leach-



Figure 24. Possible paleokarst features just southeast of the breccia pipe at study site 1 (see red arrow within the yellow oval on figure 11). (A) Extensive collapse polymictic breccia. (B) Close-up of limestone and chert breccia clasts. Note the lack of calcite veins and dolomite. (C) Red staining, possibly terra rosa weathering, at the top of the Desert Limestone near the contact with the overlying Humbug Formation(?).



Figure 25. Madison Limestone section at study site 2.

ing and dolomitization (figures 27, 28, and 29). As these processes go to greater completion, various rock types appear to have an in situ, highly brecciated fabric with apparent “clasts” or autoclasts, which have moved little from where they formed. Fractures are solution enlarged, and “clast” sizes are highly variable, chaotic, and generally angular to subangular. There is no detrital sediment infilling between the “clasts” or within solution-enlarged fractures (figure 29).

The combination of post-burial fracturing, late dissolution, and saddle dolomite replacement, followed by pyrobitumen lining of pores and fractures, is an important step in the creation of an “autobreccia” or in situ breccia within Leadville reservoirs (figure 30). Dissolution porosity formed first due to undersaturated water migrating up faults/fractures and through matrix to enhance porosity. Later, when recharging water reached saturation with respect to dolomite (under higher temperature and pressure), saddle dolomite formed as cement that reduced porosity and permeability. These processes and resulting fracture breccias are important elements of Lisbon field.

Intense bitumen plugging is concurrent or takes place shortly after brecciation (figures 27 through 31). Coarse, late replacement, saddle dolomitization and dissolution results in post-burial porosity that is marked by black pyrobitumen. Black areas between “clasts” are

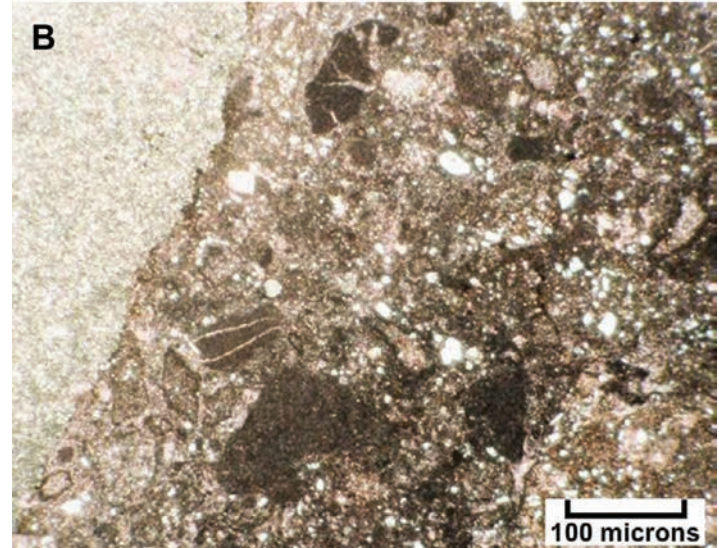


Figure 26. Megabreccia at study site 2. (A) Small-scale ooid shoal and collapse breccia (outcrop is approximately 10 feet [3 m] high). (B) Photomicrograph (plane light) showing the contact between dolomitic grainstone (light gray, upper left) and the dolomitized karst cavity filling of small carbonate clasts.

an indication of very good intercrystalline porosity as pores are lined with pyrobitumen; low porosity is represented by light gray dolomite “clasts.” These clasts are often surrounded by solution-enlarged fractures partially filled with coarse rhombic and saddle dolomites that are also coated with pyrobitumen.

Typically, black and gray core slabs show remnants of white to gray limestone that originally contained low porosity (figure 30). Processes of fracturing, saddle do-

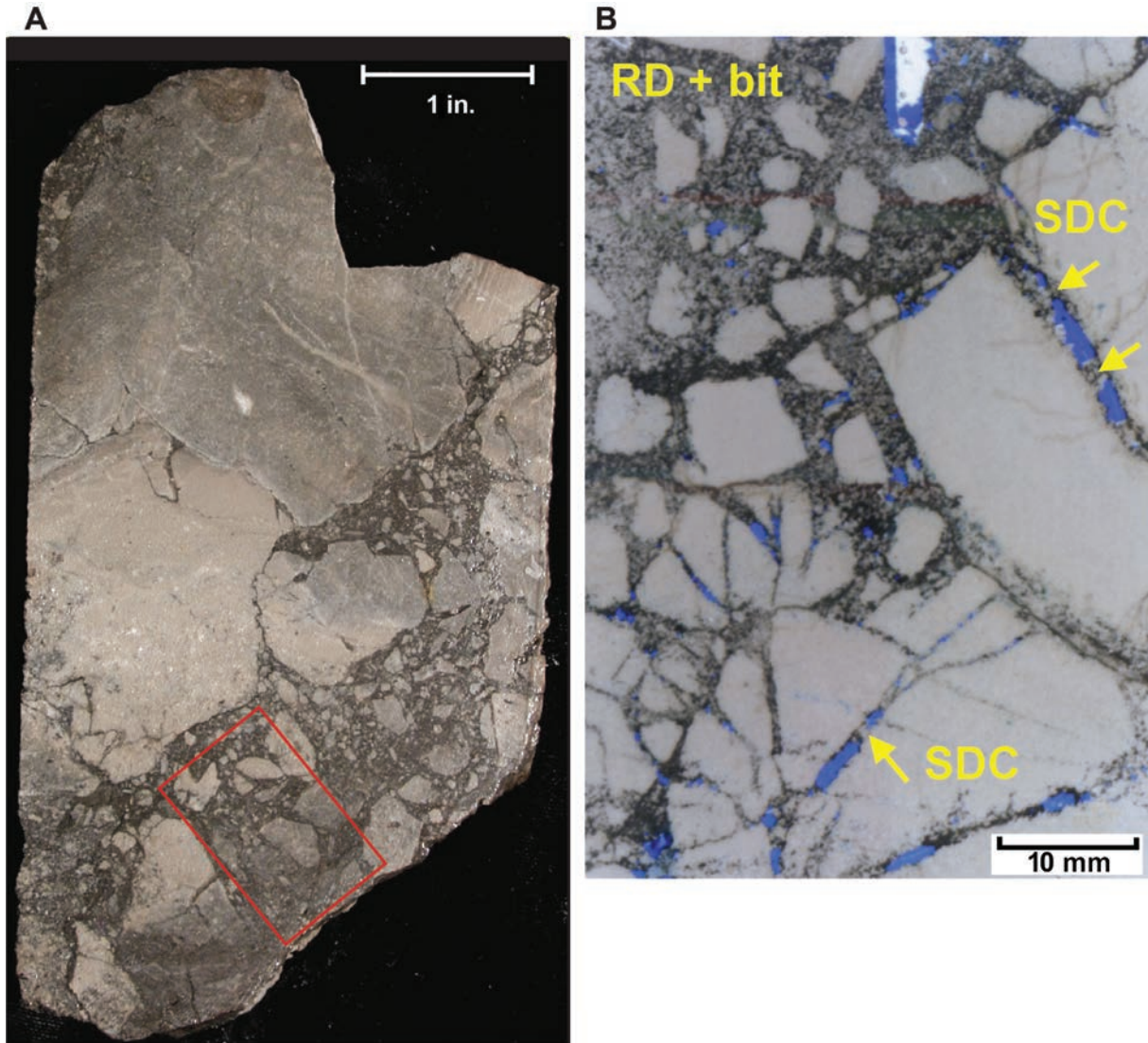


Figure 27. Autobrecciation in the Leadville Limestone from Lisbon field. (A) Core slab showing a dolomite autobreccia in which the “clasts” have moved very little. The black material surrounding the in-place “clasts” is composed of porous, late replacement dolomite coated with pyrobitumen. The red box indicates the approximate position of the thin section shown on B. (B) Entire thin section overview image (plane light) from the brecciated portion of the core shown on A, showing low-porosity, light gray dolomite “clasts” surrounded by solution-enlarged fractures partially filled with coarse rhombic dolomite (RD) and saddle dolomite that is coated with black pyrobitumen (bit). The open fracture segments (in blue) between clasts are bridged by coarse saddle dolomite crystals (SDC). Lisbon NW USA No. B-63 well (figure 6), 9938.3 feet (3029.2 m), porosity = 6.4%, permeability = 54 mD.

lomitization, leaching, and brecciation, followed by pyrobitumen coating of matrix pore systems often continue unabated leading to very porous fractured dolomite. Hence, by these processes former burial breccias appear to superficially resemble black “shales” (figure 30B). The black overprint of the original rock fabric is due to in-

tense pyrobitumen coating of pores and is observed in thin section (figure 32). Pyrobitumen rather than detrital sediment line many of the pores. These overprints can stop at healed fracture or stylolitic contacts (figure 32C). This black-rock-appearing lithofacies forms important reservoirs in Lisbon field.

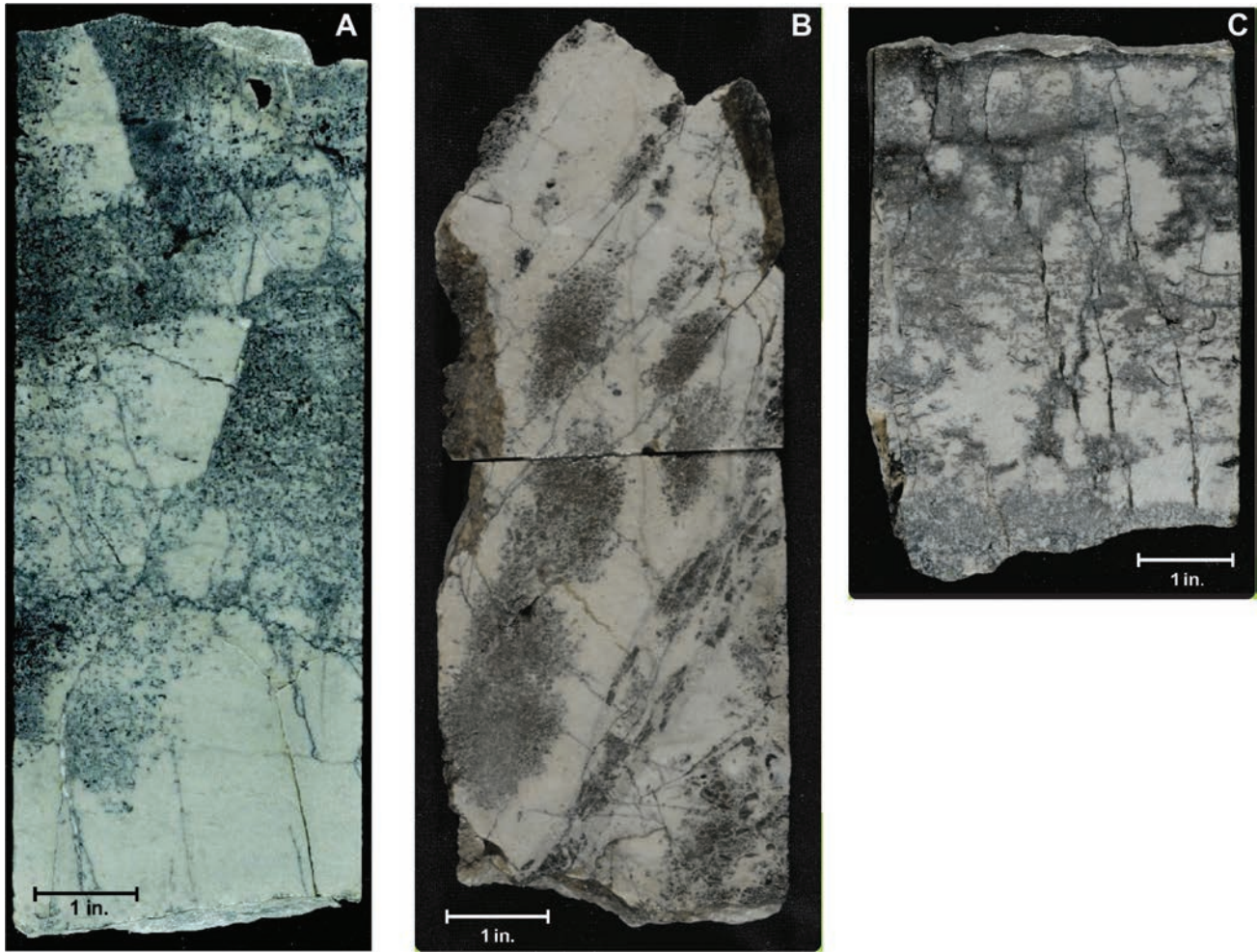


Figure 28. Autobrecciation in the Leadville Limestone from the northwestern region of the Paradox fold and fault belt. (A) Core slab showing fractures, coarse dolomitization, leaching, and the formation of breccia due to post-burial processes. Black pyrobitumen lines the significant post-burial porosity and fractures that are superimposed on a well-bedded oolitic/peloidal grainstone. Long Canyon No. 1 well (section 9, T. 26 S., R. 20 E., SLBL&M, Grand County, Utah, figure 14), 7733 feet (2357 m). (B) Core slab showing fractures, and post-burial fracture dissolution and dolomitization that results in porosity that is marked by black pyrobitumen. The fracture and dissolution create the appearance of an in situ brecciated fabric that overprints a well-bedded oolitic/peloidal grainstone. Big Flat No. 3 well (figure 14), 7790 feet (2374 m). (C) Core slab showing solution-enlarged vertical fractures, and post-burial leaching and dolomitization of a very well cemented crinoidal grainstone. The combination of the fracturing, leaching, and dolomitization in the black areas (porous areas lined with pyrobitumen) leads to the appearance of an in situ brecciated fabric. Big Flat No. 2 well (figure 14), 7784 feet (2373 m).

Late Dolomite Replacement, Saddle Dolomite, Poikilotopic Calcite, and Quartz Crystals

Petrographic analysis shows that late, coarse dolomitization, rhombic white saddle dolomites, and poikilotopic calcite (also referred to as macrocalcite) are associated with post-burial breccia (figure 33). Sad-

dle dolomite characteristically displays curved crystal shapes in thin section and sweeping extinction under cross-polarized lighting. Dissolution and fracture porosity can be filled with saddle dolomite, late poikilotopic calcite, and pyrobitumen (figure 33).

Small fluid inclusions, most of which are less than a

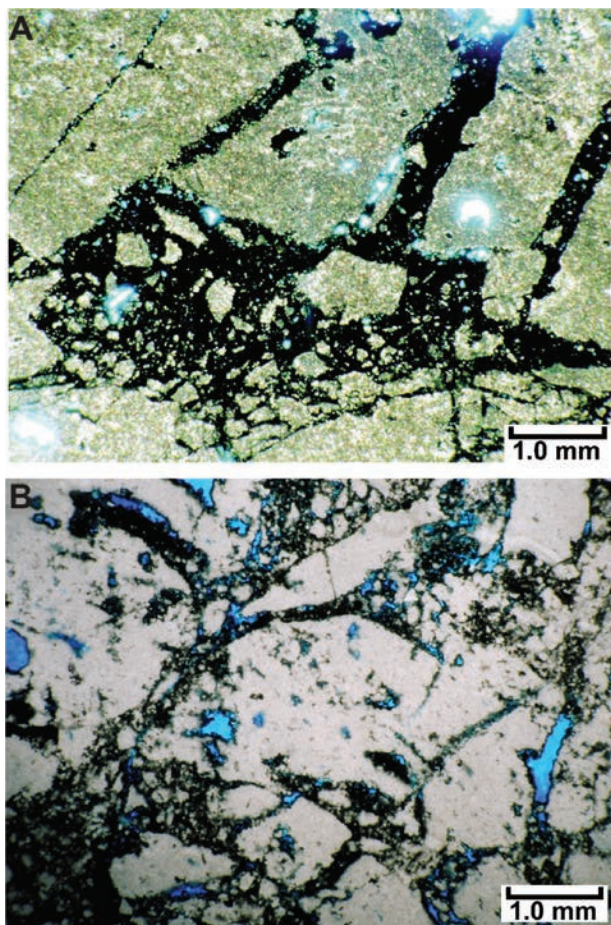


Figure 29. Photomicrographs (plane light) from a highly brecciated dolomite in which fracturing and associated dissolution have created apparent “clasts,” Lisbon field. (A) Much of the porosity in this view is lined or plugged with black pyrobitumen. Lisbon No. D-616 well (figure 6), 8579 feet (2615 m). (B) Large autoclasts and bitumen in the intensely brecciated dolomite. Note that pyrobitumen (and non-detrital sediment) lines many of the pores such that this rock is black when viewed in a core. This image was taken under plane light using the “white card technique” which makes it easier to see some of the small breccia clasts that result from intense fracturing. Lisbon No. D-816 well (figure 6), depth = 8423 feet (2567 m), porosity = 10.5%, and permeability = 47 mD.

few micrometers in length, are common in saddle dolomite. Large saddle dolomite crystals frequently contain fluid-rich, cloudy cores and fluid-poor, clear rims (figure 33), suggesting two distinct periods of dolomitization. These inclusions define growth zones and are therefore primary in origin. Both aqueous and oil inclusions are found in the saddle dolomite within the Lisbon cores

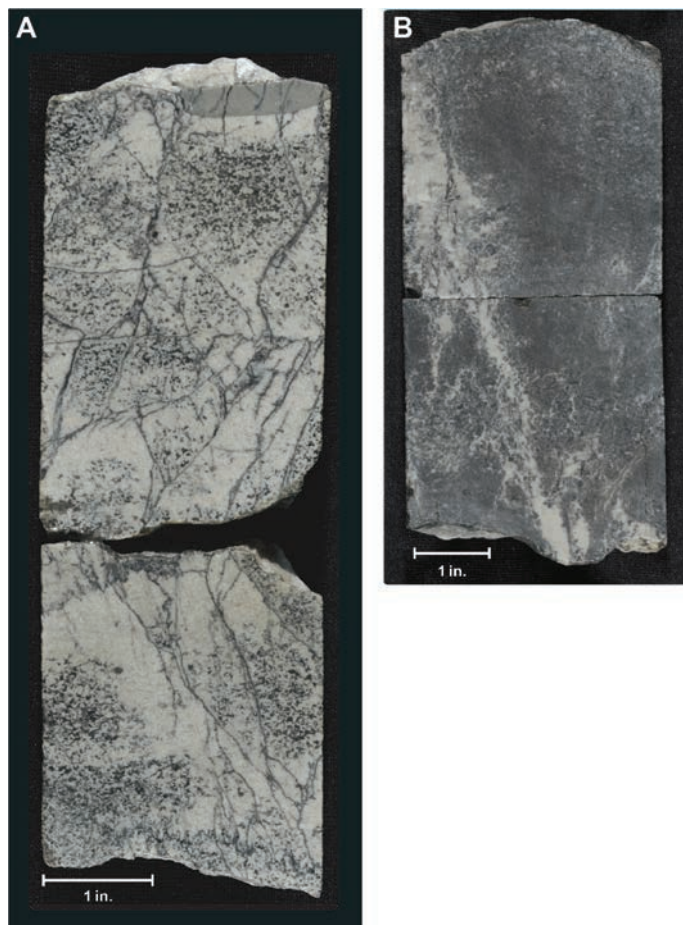


Figure 30. Core slabs showing the combination of fracturing, saddle dolomite replacement, and leaching followed by pyrobitumen lining of pores and fractures creating an in situ breccia or “autobreccia” within Leadville reservoirs. (A) An example of brecciation due to intense development of these processes within an oolitic/peloidal grainstone. Long Canyon No. 1 well (figure 14), 7732 feet (2357 m). (B) Core slab showing remnants of white limestone that originally exhibited very low porosity. By the processes listed above, the rock appears to superficially resemble a black “shale.” Big Flat No. 3 well (figure 14), 7735 feet (2358 m).

(Joseph N. Moore, Energy & Geoscience Institute, written communication, 2009), indicating sweep through the reservoir with oil-in-place. Inclusion-poor rims may have formed after movable hydrocarbons were swept from the reservoir leaving pyrobitumen behind.

Poikilotopic calcite consists of late, large, slow-growing crystals, and although not extensive in the Leadville

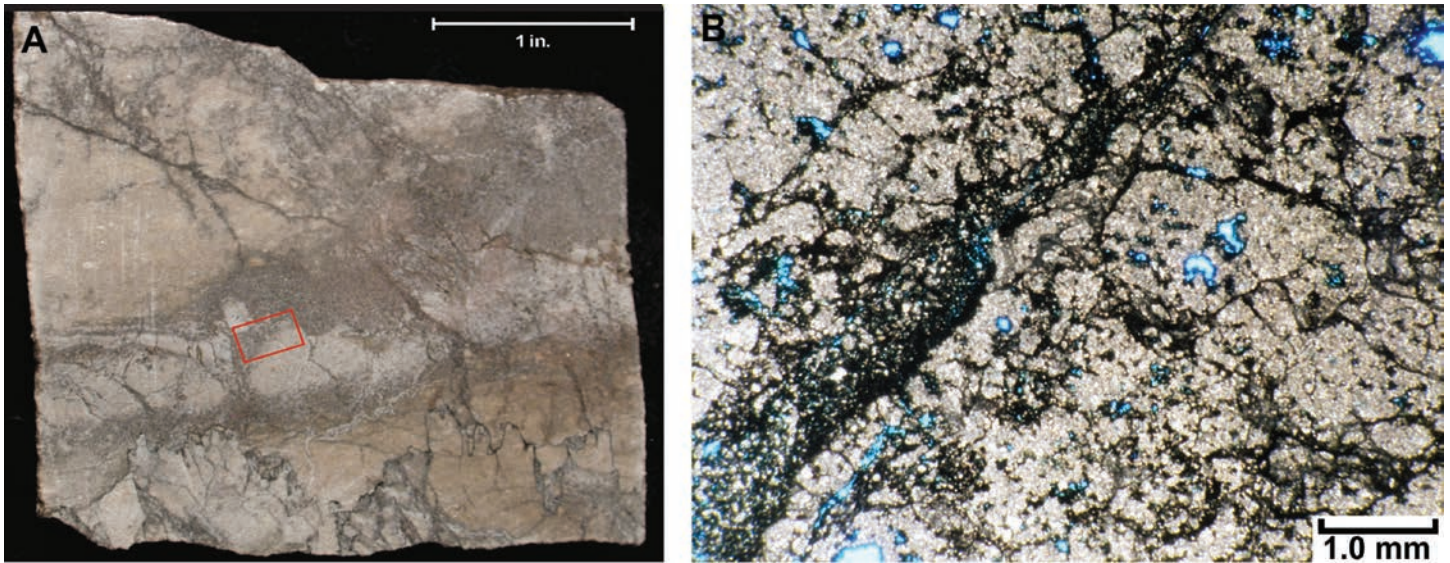


Figure 31. Brecciation in dolomite from the Leadville Limestone from Lisbon field. (A) Core slab of a dolomitized, peloidal/crinoidal packstone/wackestone with swarms of fractures marked by black, coarse dolomite. The red box indicates the approximate position of the thin section photomicrograph shown on B. (B) Representative photomicrograph (plane light) from the core in A, showing highly deformed and brecciated dolomite within a bitumen-lined fracture zone. Lisbon No. D-816 well (figure 6), 8438.5 feet (2572.1 m), porosity = 11% and permeability = 5 mD.

Limestone at Lisbon field, its presence provides some significant insight into the diagenetic history of these rocks. Examples shown in figure 33 display an autobreccia that retains small amounts of early, finely crystalline (low-permeability) dolomite replaced by “mini-saddles” and medium crystalline (euhedral) dolomite. Early during the sample’s history, it once had intercrystalline porosity that was enhanced by dissolution to form additional pores. Subsequently, the pores were partially filled with coarsely crystalline saddle dolomite and bitumen. Finally, the remaining solution-enlarged pores were occluded by poikilotopic calcite. Poikilotopic calcite may have formed as oil-field water rose through time, following the gas/condensate cap.

Scanning electron microscopy (SEM) reveals that microporosity, in the form of intercrystalline porosity, is common in the Leadville Limestone in Lisbon field. Dissolution has contributed to porosity and enhanced permeability, creating moldic, vuggy, and channel porosity, and enlarged fractures in breccias. There is a significant porosity increase where non-porous (low-permeability) early dolomites have been replaced by late, rhombic and saddle dolomites. Euhedral quartz, identi-

fied in SEM, also fills some voids within late dissolution pores and fractures (figure 34). Quartz crystals are referred to as “mini-Herkimers” (i.e., doubly terminated) and contain high-temperature fluid inclusions (Joseph N. Moore, Energy & Geoscience Institute, written communication, 2009). The presence of mini-Herkimers suggests that a high-temperature event(s) occurred in the Leadville (discussed later).

Zebra Dolomite and Rimmed Microstructures

Zebra dolomite is recognized by distinctive dark and light banding (figure 35A). Banding is parallel to bedding, with light layers coarser than darker layers. Bands range in thickness from millimeters to centimeters. Alternating dark and light bands in zebra dolomites form by dolomite replacement of original carbonate host rock and void-filling saddle dolomite (Swennen and others, 2003; Diehl and others, 2010; Wallace and Hood, 2018). Zebra dolomite is a complex late diagenetic combination of infiltration of high-temperature and pressure brines, recrystallization, dissolution, fracturing and brecciation, and fabric-selective replacement (Diehl and others, 2010; Wallace and Hood, 2018). Faulting/

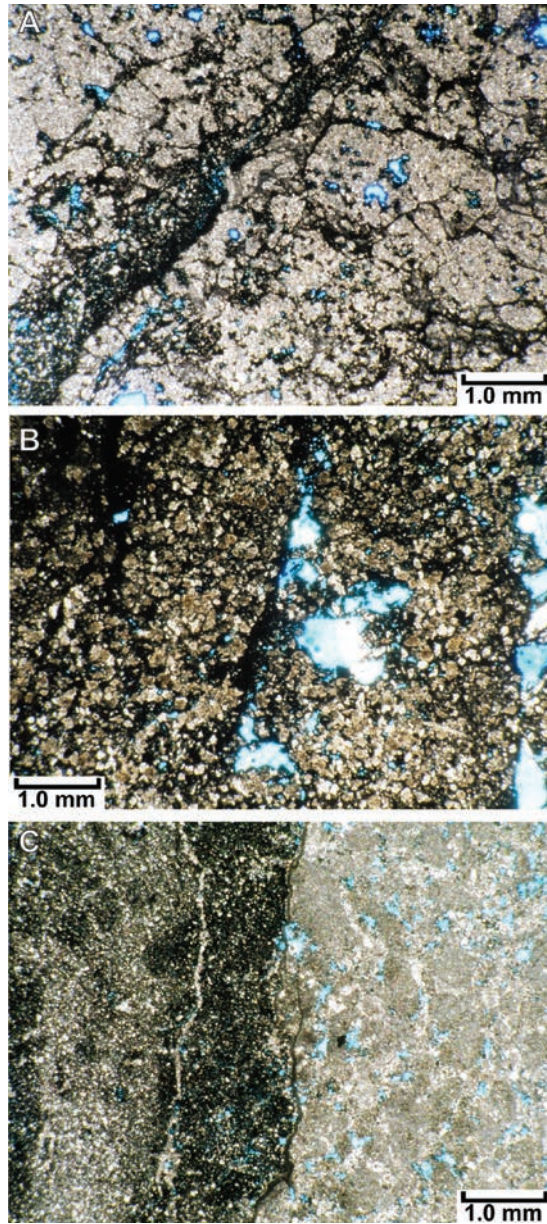


Figure 32. Photomicrographs (plane light) of a black carbonate breccia from the Lisbon No. D-816 well (figure 6), Lisbon field. (A) Intense fracture system and the brecciated “look” within a coarse dolomite. The rock looks like a black “shale” in core due to pyrobitumen lining fractures and matrix pores. Depth = 8423 feet (2567 m), porosity = 10.5%, and permeability = 47 mD. (B) Intensely fractured and dolomitized matrix. Black pyrobitumen lines open fractures and pores. Depth = 8435.8 feet (2571.2 m), porosity = 7.5%, and permeability = 0.03 mD. (C) Black overprint of a peloidal/oolitic grainstone with a well-preserved early pore system (in blue). This overprint appears to stop at a healed fracture or stylolitic contact. Depth = 7897 feet (2407 m), porosity = 6.3%, and permeability = 83 mD.

fracturing is usually a controlling factor (Swennen and others, 2003). Zebra dolomite can host economic base metal mineralization and other ore deposits.

In the Leadville Limestone, much of the dolomite associated with zebra structures is white saddle dolomite. Incipient zebra dolomite banding occurs through development of layered clusters of coarse, white, almost “pearly” saddle dolomite. Late, post-burial porosity created by saddle dolomitization and dissolution of original low-porosity limestone host rock is typically lined with black pyrobitumen producing the darker bands. Zebra dolomite can also form layered megascopic open pores or zebra vugs in coarse dolomite (figure 35B). Vertical stylolites are a product of a compressional event(s) (i.e., Laramide orogeny). These layered pore systems often terminate against and post-date both bed-parallel and bed-normal (vertical) stylolites (figure 35). Pyrobitumen lines pore space and fractures. In other intervals, zebra dolomite takes on a breccia-like appearance.

Rimmed microstructures having distinctive parallel “railroad” or stair-step fractures, are present in Leadville cores (figure 36). Associated with these fractures are replacement saddle dolomite and matrix porosity lined with pyrobitumen. They reflect shear and explosive fluid expulsion from buildup of pore pressure. Areas between clasts can exhibit very good intercrystalline porosity or microporosity or may be filled by low-porosity saddle dolomite cement. Most saddle dolomite acts as cement.

Autobrecciation in Uinta Mountain Mississippian Outcrops

Two of the three sites selected for Mississippian outcrop studies in the Uinta Mountains (figure 8) expose features attributed to autobreccia due to hydrofracturing: (1) study site 1 – South Fork Provo River (figure 11) and (2) study site 3 – Crouse Reservoir/Diamond Mountain Plateau (figure 13). Both study sites 1 and 3 have autobreccia characteristics analogous to those observed in cores of Leadville Limestone. In addition, when put into the regional stratigraphic setting, they provide a hydrologic model by which autobreccia in the Leadville may have formed.

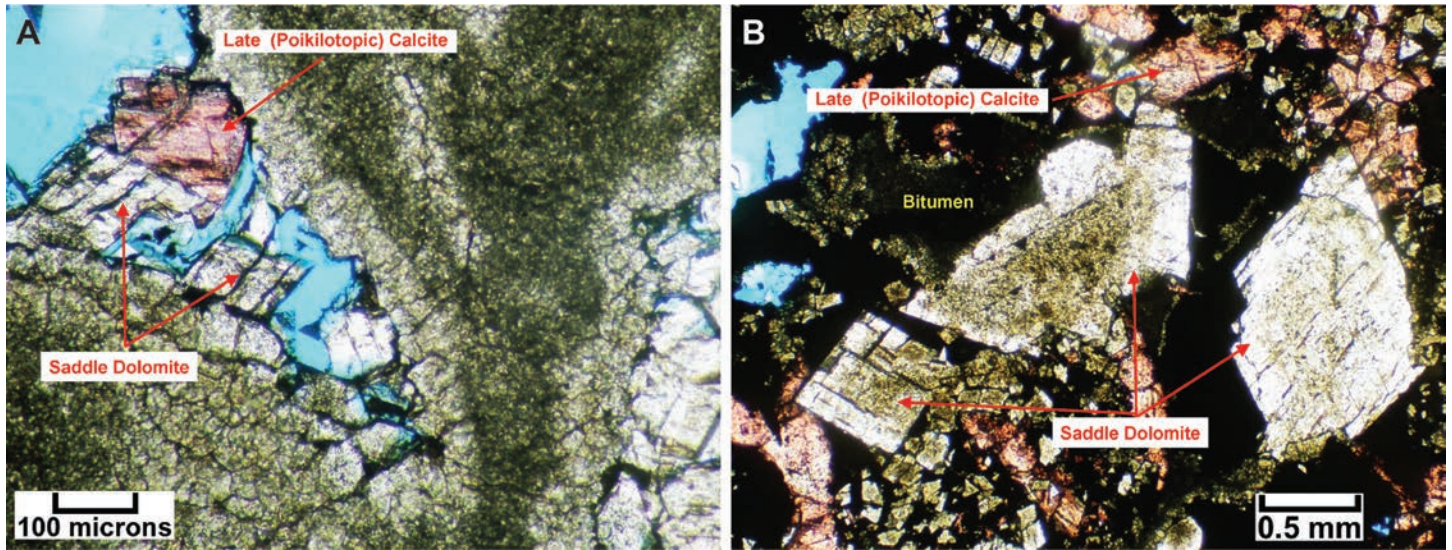


Figure 33. Photomicrographs (plane light) showing late dolomite, calcite, and pyrobitumen associated with post-burial breccia from the Northwest Lisbon No. B-63 well (figure 6), Lisbon field. (A) Coarse, white saddle dolomite crystals and a single, coarse, late calcite cement crystal (stained red) filling part of a large dissolution/fracture pore (blue) in a brecciated dolomite matrix. Depth = 9991.8 feet (3045.5 m). (B) Coarse rhombic and saddle replacement dolomite that displays cloudy cores and clear rims. The cloudy appearance is due to abundant aqueous and oil fluid inclusions. Dissolution pores are filled with pyrobitumen and late calcite (stained red). The pyrobitumen emplacement within this late porosity system gives the rock a black “shale” appearance when viewed in core. Depth = 10,005 feet (3050 m), porosity = 14.4%, and permeability = 1.9 mD.

Study Site 1 – South Fork Provo River

A large breccia pipe in the Deseret Limestone is the most striking feature at study site 1 (figure 37). A breccia pipe is a cylindrical- or irregular-shaped mass of brecciated rock. Hydrothermal breccia pipes form when hydrothermal solutions forced their way towards the surface through zones of weakness or fracture zones and naturally break up the rocks in the process (i.e., hydrofracturing); breccia pipes can also form by collapse.

The breccia pipe at study site 1 is subvertical, 17 feet (5 m) wide at the base of the outcrop, and cuts vertically through about 30 feet (9 m) of Deseret Limestone. The interior of the pipe contains poorly sorted breccia with small to large clasts surrounded by pulverized rock (figure 38A). Calcite veins, dolomitized zones, and vugs are widespread (figure 38B). Contacts of the pipe with unaltered limestone country rock are sharp. Vertical, commonly calcite-filled fractures are prevalent on both sides of the breccia pipe. Thin sections reveal the presence of mini-Herkimer quartz crystals (figure 38C), which were also found in Leadville Limestone

cores from Lisbon field (see figure 34). The presence of mini-Herkimer crystals also suggests a high-temperature event occurred at the study site, presumably emplacing the breccia pipe.

Study Site 3 – Crouse Reservoir/Diamond Mountain Plateau

The Mississippian section at study site 3, Crouse Reservoir/Diamond Mountain Plateau, is mapped as Madison Limestone. It consists of unaltered units of limestone showing cycles of three depositional environments: (1) storm-dominated, outer-shelf, crinoid shoals, (2) low-energy, open-marine, mud-rich inter-shoal (inner ramp or inner shelf), and (3) low-energy, open-marine, outer-shelf above storm wave base.

A unique feature at study site 3 is a ridge with two depressions dominated by intense breccia zones (pipes?), 75 to 100 feet (25–30 m) wide composed of highly brecciated dolomitic matrix (figures 39 and 40). The depressed zones are characterized by coarse calcite vein-like mineralization (figures 41 and 42A).

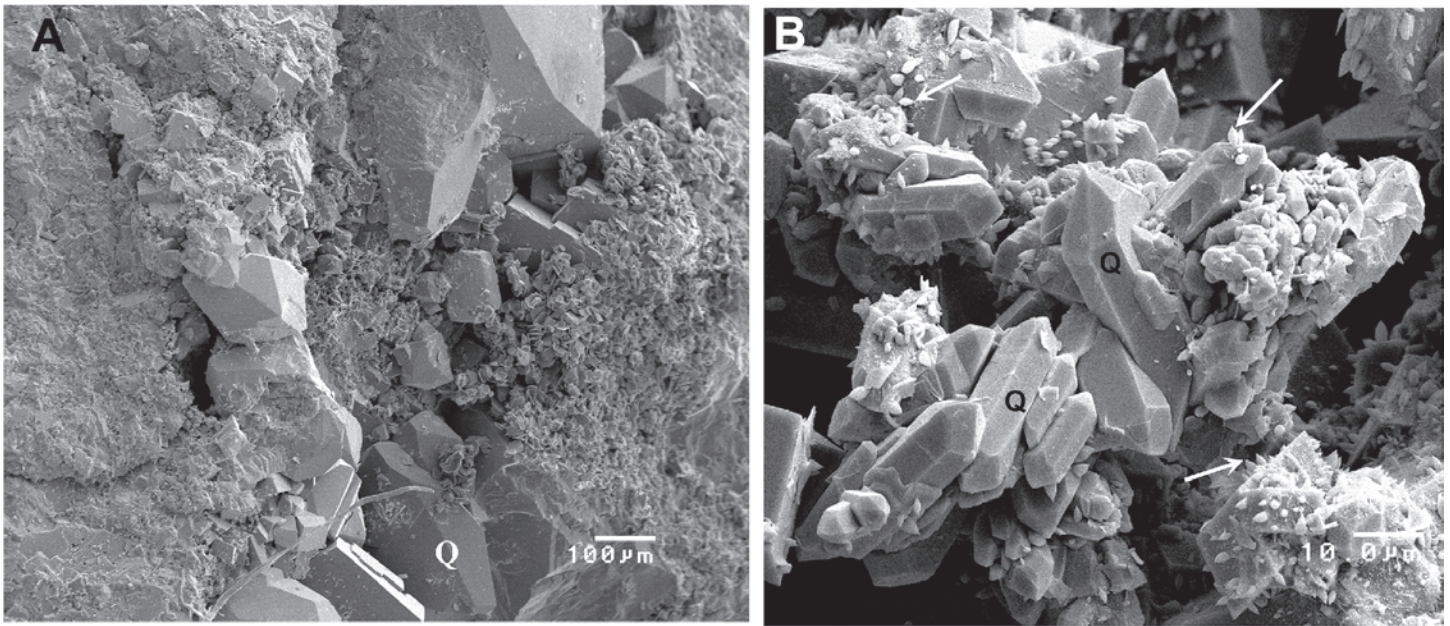


Figure 34. Scanning electron microscope photomicrograph from brecciated dolomites in Lisbon field. (A) Euhedral quartz filling voids (Q) within late dissolution pores surrounded by a dolomitized and fractured matrix. Lisbon No. D-616 well (figure 6), 8356 feet (2547 m). (B) Clusters of euhedral, doubly terminated quartz crystals (i.e., “mini-Herkimers”) (Q) from a black carbonate with intense fracturing and brecciation. The small spiky materials precipitated on many of the surfaces are either pyrobitumen or sulfide minerals (arrows). Lisbon No. D-816 well (figure 6), 8486 feet (2587 m).

Dolomitization and leaching of matrix limestone has occurred throughout these zones (figure 42B). These distinctive elements imply a hydrothermal event rather than a paleokarst collapse origin for the breccia zones.

Discussion

Similar depositional environments described from outcrops above are also observed in Leadville cores from Lisbon field. Carbonate buildups containing good porosity/permeability are the best reservoir analog units, whereas low-porosity/permeability, open-marine packstones and wackestones represent less attractive reservoir analog units, unless they have experienced dolomitization in the subsurface that improved reservoir quality. Breccia pipes, paleokarst, and fractures also enhance reservoir quality. Post-burial breccias associated with hydrothermal events, fracturing, and dissolution in the Leadville Limestone yield the best reservoirs at Lisbon field.

Model for Post-Burial Brecciation in Uinta Mountain Mississippian Outcrops

Breccia pipes and zones discovered at study sites 1 and 3 are likely the result of hydrothermal activity in the geologic past. The presence of the basal Cambrian Tintic Quartzite in the southern flank of the western Uinta Mountains (figure 9) and the stratigraphically equivalent Lodore Formation in the eastern part of the range (figure 10) may serve as hydrothermal recharge aquifers and are important contributors to the hydrothermal story. The Tintic Quartzite is a very coarse to granular sandstone with moderately sorted, subrounded to spherical, monocrystalline and polycrystalline quartz grains. The Tintic has thin to thick cross-bedding, is moderately indurated, and contains a few shale partings, which have small amounts of mica and some biogenic feeding trails (Dockal, 1980). The contact of the Tintic with overlying Mississippian strata is sharp. The Lodore is a very fine to medium-grained, well-sorted, very thin bedded to cross-bedded (with undulato-



Figure 35. Zebra dolomite structures in the Leadville Limestone from the northwestern region of the Paradox fold and fault belt. (A) Core slab of zebra dolomite showing distinctive black and white bands that are the result of coarse white saddle dolomite replacement and vug development in layers as well as dissolution of rock matrix with black pyrobitumen lining pores. The zebra banding stops against and probably post-dates a bed-parallel stylolite at the base of this segment (between arrows). Floy No. 1 Salt Wash well (figure 14), 9647 feet (2940 m). (B) Core slab showing the host rock consisting of well-cemented peloidal/oolitic grainstone with extensive development of zebra vugs and layered zebra dolomite in the right-hand portion of the slab that abuts against a vertical (bed normal) stylolite (see arrows). Long Canyon No. 1 well (figure 14), 7745 feet (2361 m).



Figure 36. Core slab showing a variety of fracture types, including rimmed microstructures with their distinctive parallel “railroad” or stair-step appearance (see examples between arrows). Long Canyon No. 1 well (figure 14), 7728 feet (2356 m).



Figure 37. Large breccia pipe cross-cutting the Desert Limestone at study site 1. Note pulverized nature of the material that comprises the pipe, the sharp contact with the country rock, and parallel, calcite-filled vertical fractures.

ry surfaces) sandstone marked by argillaceous partings (figure 43); quartz grains are subrounded to spherical. The Lodore can be calcareous and slightly ferruginous; the top appears to be eroded (Dockal, 1980). Both the Lodore and Tintic contain porous and permeable units. As aquifers, they likely supplied hot water to a former hydrothermal system.

Three-dimensional numerical models of seafloor hydrothermal convection by Coumou and others (2008) demonstrated that convection cells organize themselves into pipe-like upflow zones surrounded by narrow zones of warm downflow. Recharge can occur over an extensive area or along faults as water migration pathways. The Tintic Quartzite is mapped on the western end of the Uinta Mountains whereas the Lodore Formation is present on the eastern end. Through the central part of the southern flank of the Uinta Mountains, porous Cambrian sandstone is absent and Mississippian strata lie unconformably on Precambrian (middle Neoproterozoic) Red Pine Shale and older formations of the Uinta Mountain Group (as observed in Whiterocks Canyon [figure 8]). No hydrothermal breccia zones or pipes are found in the central part of the southern flank, lending credence to the concept that aquifers in the Tintic and Lodore were a required condition for past

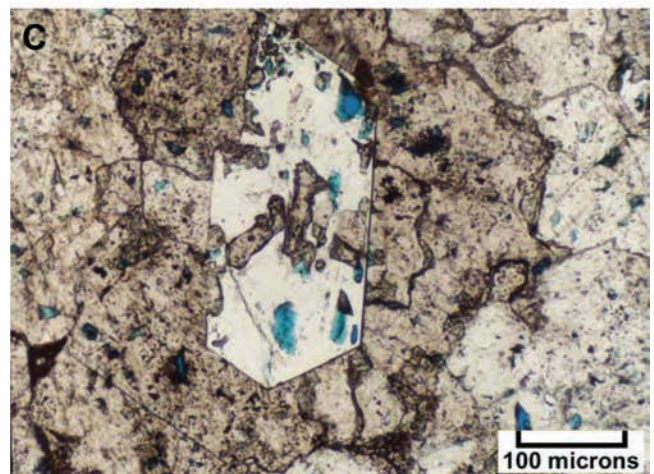


Figure 38. Characteristics of the explosive hydrothermal breccia pipe at study site 1. (A) Brecciated rock in shattered-looking, pulverized groundmass. (B) Close-up of sharp contact with unaltered limestone country rock. Note vuggy dolomite and white calcite veins. (C) Photomicrograph (plane light) of dolomite containing a mini-Herkimer quartz crystal (center) suggesting a high-temperature event.



Figure 39. Topographic depressions at the sites of major breccia zones (pipes?) along a ridge of Madison Limestone (view to the southeast).

hydrothermal activity. After pressure builds up to a certain point, the hydrothermal fluids within the aquifer can very rapidly and explosively break through zones of weakness at the intersections of fractures or along faults; this can occur as a single event or over several stages. Thus, when targeting the Leadville Limestone in the Paradox Basin for potential hydrothermal dolomite and enhanced reservoir quality due to natural hydrofracturing, the presence of an underlying aquifer and fracture zones or faults may be necessary ingredients, supported in part from what can be observed from the breccia zones at study site 1 and 3.

Strontium Isotope Geochemistry from Post-Burial Breccias, Leadville Limestone

Strontium (Sr) isotope analysis is used as a dating tool in marine carbonates. Strontium composition of ancient seawater and its variation through geologic time has been determined from common marine carbonate minerals, especially calcite, aragonite, and dolomite (Brass, 1976; Burke and others, 1982; Allan and Wiggins, 1993). The ratio of $^{87}\text{Sr}/^{86}\text{Sr}$ is the most useful for tracking the secular changes of seawater Sr. These two isotopes come from separate sources in the earth. Strontium-87 is radiogenic (from the radioactive decay of rubidium-87 with a half-life of about 50 billion

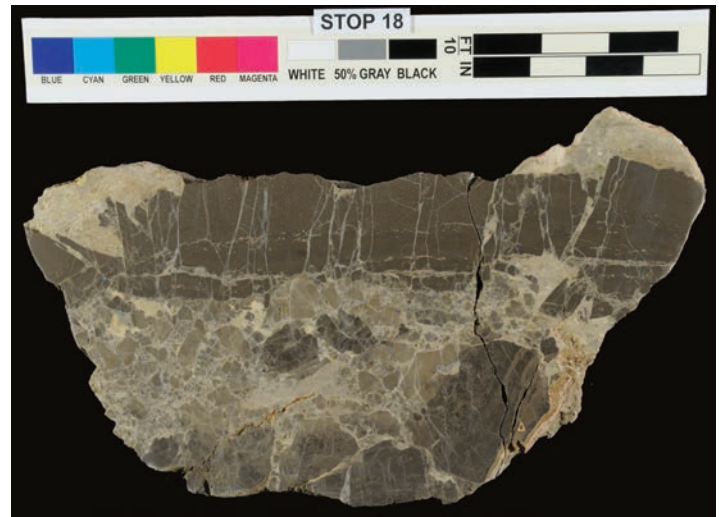


Figure 40. Slabbed specimen of highly brecciated rock typical of deposits present at study site 3.

years), whereas strontium-86 is non-radiogenic (Faure and Powell, 1972; Faure, 1977).

Strontium isotopic ratios for three Leadville samples (late calcite, saddle dolomite, and sucrosic matrix dolomite) from Lisbon field were plotted on the Phanerozoic marine carbonate curve for $^{87}\text{Sr}/^{86}\text{Sr}$ ratios (figure 44). Leadville samples are more radiogenic than accepted values for marine carbonate minerals derived from seawater sources in the Phanerozoic. The source of these radiogenic Sr ratios may have been from fluids that interacted with basement granites. Leadville $^{87}\text{Sr}/^{86}\text{Sr}$ ratios are also similar to numerous publications on radiogenic saddle dolomites in diverse Paleozoic reservoirs of North America.

Burial History and Temperature Profiles for Post-Burial Diagenesis in the Leadville Limestone

Burial history and temperature profiles for the Leadville Limestone at Lisbon field provide some guidance as to when tectonic, diagenetic, and porosity-forming events occurred (figure 45). As discussed in previous sections, saddle dolomite, euhedral quartz, pyrobitumen, and late calcite are all components of post-burial breccias, fractured zones, and major porosity intervals within Lisbon and other nearby Leadville fields.

In addition to the calculated temperature profile,



Figure 41. Breccia zone at study site 3. (A) Coarse calcite vein in a highly brecciated dolomitic matrix. (B) Close-up of large, representative calcite crystals within the dolomitic matrix of the breccia zone.

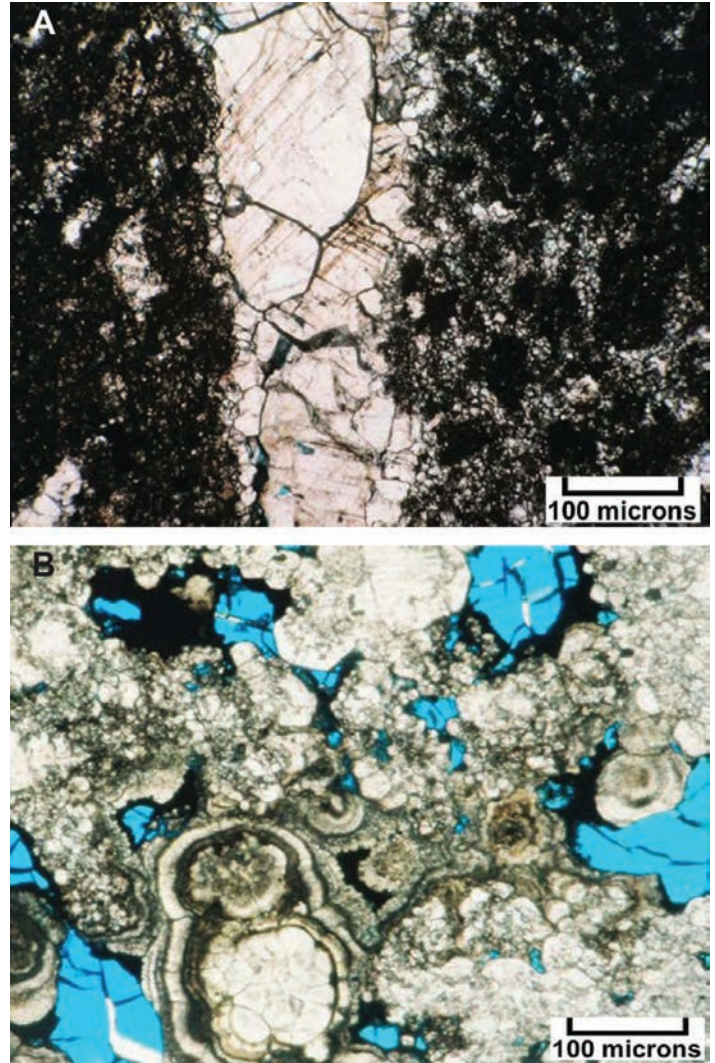


Figure 42. Photomicrographs (plane light) from breccia samples at study site 3. (A) Vein of coarse calcite in a low-permeability dolomitic matrix. (B) Unusual concentric dolomite cement (high temperature?) overgrowths in a dolomitic breccia matrix.

we have inferred anomalous temperature spikes for: (1) maximum burial, (2) late Laramide reactivation along normal faults that extend to basement, and (3) Oligocene igneous events, such as emplacement of the nearby La Sal and Abajo laccolith complexes, 10 miles (16 km) north and 23 miles (37 km) southwest, respectively, of Lisbon field (figure 1). Temperature spikes may be responsible for quartz precipitation, sulfide mineralization, pyrobitumen formation, late dissolution of carbonates, late saddle dolomite cements, and providing a heat source for hydrothermal solutions that cause au-

tobrecciation. However, vertical (bed-normal) stylolites that pre-date much of the zebra dolomite banding and zebra vug porosity as well as some brecciation were probably the result of Laramide compression.

Proposed Model for Fault-Controlled, Post-Burial Brecciation, Dolomitization, and Porosity Development, Lisbon Field

We propose a model with convection cells bound by basement-rooted faults to transfer heat and flu-



Figure 43. Basal Cambrian Lodore Formation. (A) Outcrop of thin-bedded Lodore Formation north of study site 3, southwest of Crouse Reservoir. (B) Lodore Formation hand sample of very fine grained, well-sorted, cross-bedded, slightly ferruginous sandstone.

ids possibly from crystalline basement, Pennsylvanian evaporites, and Oligocene igneous complexes. Large volumes of water are required to produce the brecciation and amount, type, and generations of dolomite present at Lisbon field. There is probably not enough water moving through the regional hydrodynamic system to account for the Leadville dolomite. Therefore, convection or circulation cells would be much larger from surface feeder systems into the subsurface, most likely sweeping through igneous intrusives and basement to acquire heat, and form circulation systems. Fault movement at various scales provided the power to pressure up and move fluids throughout the subsurface. Recycling hot, brine-bearing water in convection cells may have driven dolomitization.

A diagrammatic south to north cross section of the greater Lisbon field area (figure 46) shows possible convection cells of the circulation model for ascending warm fluids responsible for saddle dolomite (also see block diagram on figure 4B), high-temperature quartz, pyrobitumen, aggressive dissolution of limestone and dolomite, and sulfide mineralization. The basal aquifer for inferred fault-controlled cells could be the Devonian McCracken Sandstone, similar to the Lodore Formation in the Uinta Mountains. The McCracken is locally porous enough to produce oil at Lisbon field. Source of heat may have been Precambrian basement rocks and/or Oligocene igneous intrusives. Mapped faults cutting Lisbon field may have been involved with thermal convection cells circulating fluids during late burial diagenesis (figure 47). Wells near faults appear to have better reservoir quality, produce greater volumes of oil, and have higher residual bottom-hole temperatures than wells away from these faults.

CONCLUSIONS

Two distinctive types of breccias—(1) karst-related, and (2) and post-burial “autobreccias” (created by hydrofracturing)—are encountered within the Mississippian Leadville Limestone in Lisbon and nearby fields in the Paradox Basin fold and fault belt.

- Karst-related breccias are intimately associated with cave-filling detrital sediments. Karst cave-filling sedimentary facies classified by Evans and Reed (2006, 2007) for the Leadville from Colorado outcrops were identified in cores within Lisbon and other nearby fields.
- Porosity associated with karst breccias, cave-filling detrital sediments, and dolomitized carbonate cave-filling sediments is low. Cave-filling sediments disrupt lateral flow continuity within porous or fractured Leadville hydrocarbon reservoirs.
- Post-burial breccias occur within fracture swarms and singular faults/fractures. Their origin is caused by natural hydrofracturing in the subsurface. Breccias (or “autobreccias”) form in association with zebra structures, vugs, coarse

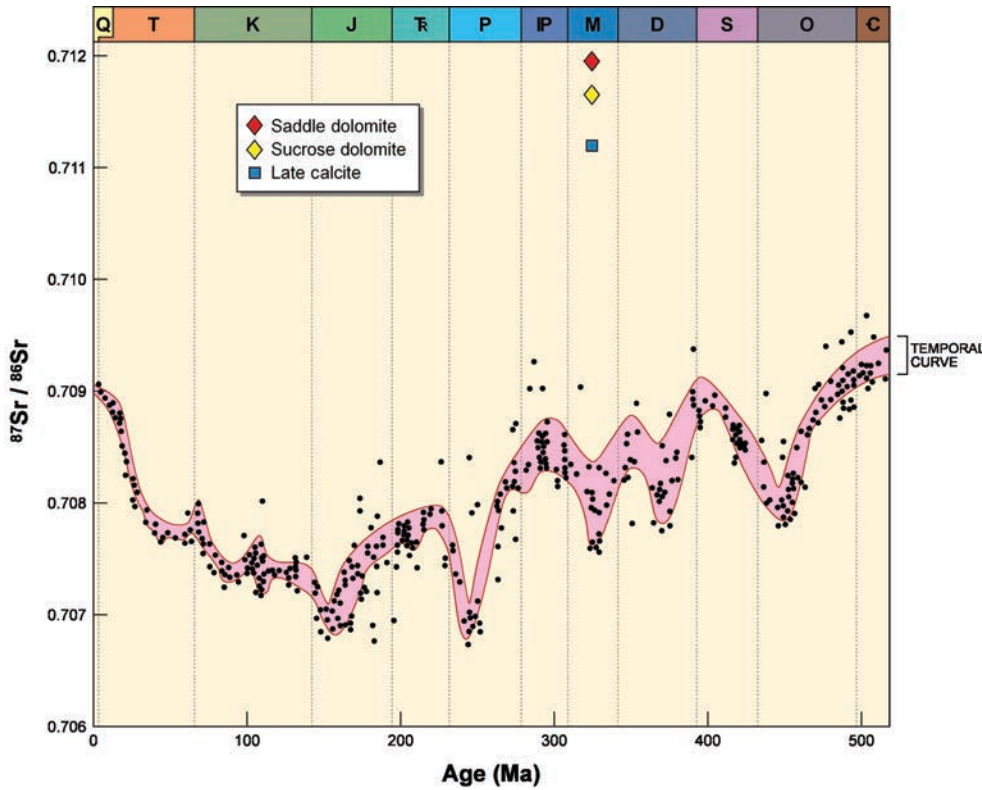


Figure 44. Strontium isotope seawater composition curve with Leadville Limestone late calcite, saddle dolomite, and sucrosic matrix dolomite samples from Lisbon field plotted for comparison. Modified from Burke and others (1982), Elderfield (1986), and Allan and Wiggins (1993).

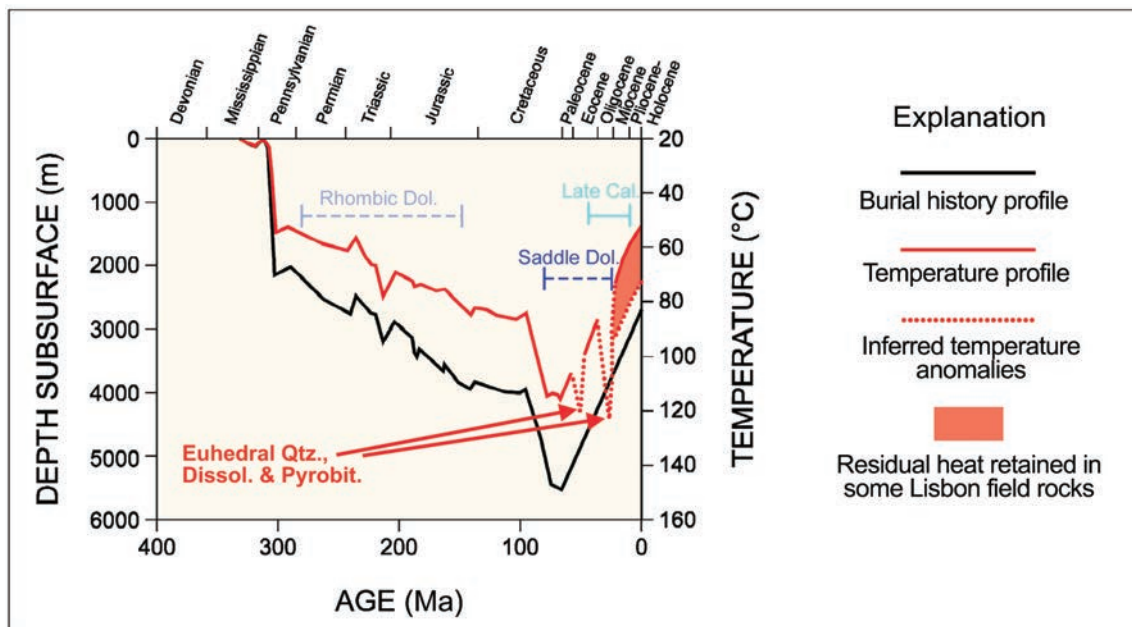


Figure 45. Burial history and temperature profiles with inferred diagenetic windows at Lisbon field.

saddle dolomite, and extensive late dissolution of host rock. Breccias and zebra structures in Leadville fields post-date vertical (bed normal) stylolites that formed during Laramide compression.

- Porosity associated with post-burial breccias and saddle dolomite in the Lisbon field area is high. However, porosity is difficult to appreciate on core slab surfaces because abundant pyro-

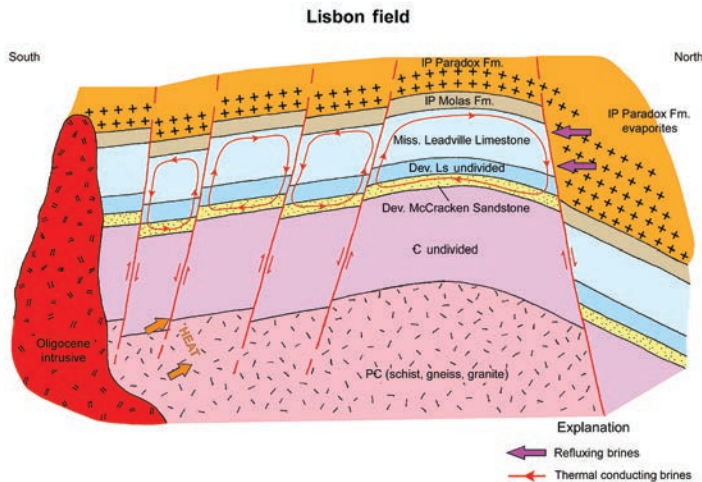


Figure 46. Possible heat sources and convection cells for late dolomitization and brecciation of the Leadville Limestone focused along high-angle faults that reach basement in the Lisbon field area.

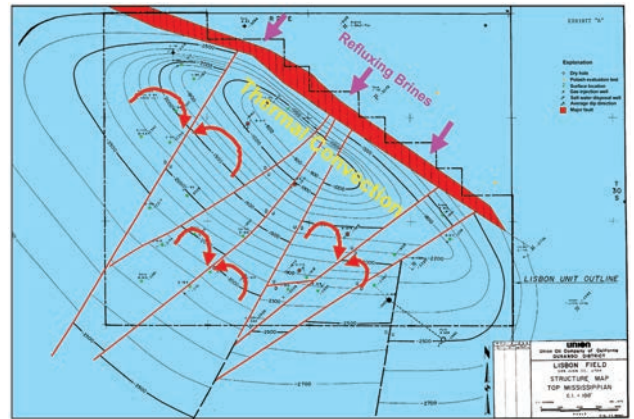


Figure 47. Top of structure of the Leadville Limestone, Lisbon field, showing possible thermal convection cells between small, northeast-southwest-trending normal faults that probably go to basement. Modified from C.F. Johnson, Union Oil Company of California files (1970) courtesy of Tom Brown, Inc.

bitumen makes porous breccias and dolomites appear like black “shales.”

- Strontium isotope ratios and associated minerals found within post-burial breccias and saddle dolomite indicate a likely fluid source that interacted with basement rocks in the area. These results show similarities to published studies on radiogenic saddle dolomites in diverse Paleozoic reservoirs throughout North America.
- The Desert and Madison Limestones in the Uinta Mountains contain local zones of breccia due to either collapse or natural hydrofracturing. Breccia associated with sediment-filled collapsed cavities is common. These cavities are related to paleokarstification of the Desert/Madison when subaerially exposed during Late Mississippian time. Brecciation caused by explosive natural hydrofracturing created similar shattered-looking, pulverized rock identified in Lisbon cores. Breccia pipes are related to past hydrothermal activity.
- The basal Cambrian Tintic Quartzite and Lodore Formation were important contributors to the

hydrothermal story. They served as aquifers to supply hot water to the hydrothermal system. Through the central part of the southern flank of the Uinta Mountains, porous Cambrian sandstone units are absent, with Mississippian strata lying unconformably on middle Neoproterozoic Red Pine Shale. No Mississippian hydrothermal breccia zones or pipes are found in the central part of the southern flank, lending credence to the concept that aquifers below in the Tintic and Lodore may be a required condition for past hydrothermal activity to have occurred. Thus, targeting Leadville Limestone areas for potential hydrothermal dolomite and enhanced reservoir quality due to hydrofracturing may require an aquifer below as a necessary ingredient (i.e., the Devonian McCracken Sandstone).

- Large volumes of water were required to produce brecciation and amount, type, and generations of dolomite present at Lisbon field. We propose a model where convection cells bounded by basement-rooted faults transferred heat and fluids possibly from crystalline basement, Pennsylvanian evaporites, and Oligocene igneous complexes.

- Breccias and associated late porosity and pyrobitumen pore coatings in fields like Lisbon may be best found or developed using a structural model involving fault geometry and fracturing rather than attempting to identify major subaerial exposure surfaces such as at the top of the Leadville Limestone. Exploration methodology using seismic attributes focused on identifying high-angle, basement-penetrating fault systems and fracture trends with attendant porosity indicators related to hydrothermal dolomitization should lead to greater success in Mississippi-an exploration of the Paradox Basin and other analogous brecciated carbonate reservoirs.

ACKNOWLEDGMENTS

Funding for this research was provided as part of the Advanced and Key Oilfield Technologies for Independents (Area 2 – Exploration) Program of the U.S. Department of Energy, National Energy Technology Laboratory, Tulsa, Oklahoma, contract number DE-FC26-03NT15424. Support was also provided by the Utah Geological Survey (UGS) and Eby Petrography & Consulting, Inc., Denver, Colorado.

Cheryl Gustin and James Parker of the UGS drafted figures. Core photography was conducted by Ammon McDonald of the UGS. Michael D. Laine and Thomas Dempster assisted with core preparation and data collection from the Utah Core Research Center.

This paper was carefully reviewed by Robert F. Lindsay, Lindsay Consulting LLC and Affiliate Professor, Brigham Young University; and David E. Tabet, Robert Ressetar, Michael D. Vanden Berg, Stephanie M. Carney, Michael D. Hylland, and Bill Keach of the UGS, along with the editors of this publication. Their suggestions and constructive criticism greatly improved the manuscript.

REFERENCES

Ahr, W.M., 1989, Mississippian reef facies in the Southwest—a spectrum of variations in depositional style and reservoir characteristics: Ft. Worth Geological Society and Texas Christian University, Symposium on the Petroleum Geology of Mississippian Carbonates in North Central Texas, p. 1–19.

- Allan, J.R., and Wiggins, W.D., 1993, Dolomite reservoirs—geochemical techniques for evaluating origin and distribution: American Association of Petroleum Geologists, Continuing Education Course Note Series 36, 129 p.
- Baars, D.L., 1966, Pre-Pennsylvanian paleotectonics—key to basin evolution and petroleum occurrences in the Paradox Basin, Utah and Colorado: American Association of Petroleum Geologists Bulletin, v. 50, no. 10, p. 2082–2111.
- Blakey, R., and Ranney, W., 2008, Ancient landscapes of the Colorado Plateau: Grand Canyon, Grand Canyon Association, p. 21–27.
- Brass, G.W., 1976, The variation of the marine $^{87}\text{Sr}/^{86}\text{Sr}$ ratio during Phanerozoic time—interpretation using a flux model: *Geochimica et Cosmochimica Acta*, v. 40, p. 721–730.
- Bryant, B., 1990, Geologic map of the Salt City 30' x 60' quadrangle, north-central Utah and Uinta County, Wyoming: U.S. Geological Survey Miscellaneous Investigations Map I-1944, 2 plates, scale 1:100,000.
- Burke, W.H., Denison, R.E., Heatherington, E.A., Koepnick, R.B., Nelson, H.F., and Otto, J.B., 1982, Variation of seawater $^{87}\text{Sr}/^{86}\text{Sr}$ throughout Phanerozoic time: *Geology*, v. 10, p. 516–519.
- Carey, M.A., 1973, Chesterian-Morrowan conodont biostratigraphy from northeastern Utah: Salt Lake City, University of Utah, M.S. thesis, 83 p.
- Chidsey, T.C., Jr. (editor and compiler), in press, The Mississippian Leadville Limestone oil and gas play, Paradox Basin, southeastern Utah and southwestern Colorado—Lisbon field, regional, and analog studies: *Utah Geological Survey Bulletin*.
- Chidsey, T.C., Jr., and Eby, D.E., 2016, Chapter 9—Mississippian Leadville Limestone Paradox Basin play, in Chidsey, T.C., Jr., editor, Major oil plays in Utah and vicinity: *Utah Geological Survey Bulletin* 137, p. 145–157.
- Chidsey, T.C., Jr., Morgan, C.D., and Eby, D.E., 2016, Chapter 10—Pennsylvanian Paradox Formation Paradox Basin play, in Chidsey, T.C., Jr., editor, Major oil plays in Utah and vicinity: *Utah Geological Survey Bulletin* 137, p. 159–206.
- Clark, C.R., 1978, Lisbon, San Juan County, Utah, in Fassett, J.E., editor, Oil and gas fields of the Four Corners area: *Four Corners Geological Society*, v. II, p. 662–665.
- Coumou, D., Driesner, T., and Heinrich, A., 2008, The structure and dynamics of mid-ocean ridge hydrothermal system: *Science Magazine*, v. 321, p. 1825–1828.
- Davies, G.R., 2004, Hydrothermal (thermobaric) dolomite and leached limestone reservoirs—general principles, genetic connections, and economic significance in Canada [abs.]: American Association of Petroleum Geologists Annual Convention, Official Program with Abstracts, v. 13, p. A32.
- Davies, G.R., and Smith, L.B., Jr., 2006, Structurally controlled hy-

- drothermal alteration of carbonate reservoirs—an overview: American Association of Petroleum Geologists Bulletin Special Issue—Hydrothermally Altered Carbonate Reservoirs, v. 90, no. 11, p. 1641–1690.
- Diehl, S.F., Hofstra, A.H., Koenig, A.E., Emsbo, P., Christiansen, W., and Johnson, C., 2010, Hydrothermal zebra dolomite in the Great Basin, Nevada—attributes and relation to Paleozoic stratigraphy, tectonics, and ore deposits: *Geosphere*, v. 6, no. 5, p. 663–690.
- Dockal, J.A., 1980, Petrology and sedimentary facies of Redwall Limestone (Mississippian) of Uinta Mountains, Utah and Colorado: Iowa City, Iowa State University, Ph.D. dissertation, 423 p.
- Eby, D.E., Chidsey, T.C., Jr., and Sprinkel, D.A., 2014, Marine microbial carbonate facies, fabrics, and petroleum reservoirs in Utah [abs.]: Geological Society of America Rocky Mountain/Cordilleran Section Abstracts with Program, v. 46, no. 5, p. 12.
- Elderfield, H., 1986, Strontium isotope stratigraphy, in Shackleton, N.J., editor, Boundaries and events in the Paleogene: Paleogeography, Paleoclimatology, Paleocology, v. 57, p. 71–90.
- Eskelsen, Q.M., 1953, Geology of the Soapstone Basin and vicinity, Wasatch, Summit, and Duchesne Counties, Utah: Salt Lake City, University of Utah, M.S. thesis, 56 p., 2 plates, scale 1:31,680.
- Evans, J.E., and Reed, J.M., 2006, Pennsylvanian fluvial cave sediments in the Mississippian Leadville Limestone, southwestern Colorado, U.S.A.: *The Mountain Geologist*, v. 43, no. 4, p. 283–297.
- Evans, J.E., and Reed, J.M., 2007, Integrated loessite—paleokarst depositional system, early Pennsylvanian Molas Formation, Paradox Basin, southwestern Colorado, U.S.A.: *Sedimentary Geology*, v. 195, p. 161–181.
- Faure, G., 1977, Principles of isotope geology: New York, John Wiley and Sons, 464 p.
- Faure, G., and Powell, J.L., 1972, Strontium isotope geology: Berlin, Springer Verlag, 188 p.
- Fouret, K.L., 1982, Depositional and diagenetic environment of the Mississippian Leadville Formation at Lisbon field, Utah: College Station, Texas A&M University, M.S. thesis, 119 p.
- Fouret, K.L., 1996, Depositional and diagenetic environment of the Mississippian Leadville Limestone at Lisbon field, Utah, in Huffman, A.C., Jr., Lund, W.R., and Godwin, L.H., editors, Geology and resources of the Paradox Basin: Utah Geological Association Publication 25, p. 129–138.
- Godfrey, A.E., 1985, Karst hydrology of the south slope of the Uinta Mountains, Utah, in Picard, M.D., editor, Geology and energy resources, Uinta Basin of Utah: Utah Geological Association Publication 12, p. 277–293.
- Hill, C.A., and Forti, P., 1997, Cave minerals of the World: Huntsville, Alabama, National Speleological Society, Inc., 463 p.
- Hintze, L.F., and Kowallis, B.J., 2009, Geologic history of Utah: Provo, Utah, Brigham Young University Geology Studies Special Publication 9, 225 p.
- Hintze, L.F., Willis, G.C., Laes, D.Y.M., Sprinkel, D.A., and Brown, K.D., 2000, Digital geologic map of Utah: Utah Geological Survey Map 179DM, scale 1:500,000.
- Johnson, C.F., 1970, Top of structure of the Leadville Limestone, Lisbon field: unpublished map, Union Oil Company of California files.
- Lees, A., and Miller, J., 1995, Waulsortian banks, in Monty, C.L.V., Bosence, D.W.J., Bridges, P.H., and Pratt, B.R., editors, Carbonate mud-mounds—their origin and evolution: International Association of Sedimentologists Special Publication No. 23, p. 191–271.
- Loucks, R.G., 1999, Paleocave carbonate reservoirs—origins, burial depth modifications, spatial complexity, and reservoir implications: American Association of Petroleum Geologists Bulletin, v. 83, p. 1795–1834.
- Mayo, A.L., Herron, D., Nelson, S.T., Tingey, D.G., and Tranel, M.J., 2010, Geology and hydrology of Timpanogos Cave National Monument, Utah, in Sprinkel, D.A., Chidsey, T.C., Jr., and Anderson, P.B., editors, Geology of Utah's parks and monuments: Utah Geological Association Publication 28 (third edition), p. 269–283.
- McDougald, W.D., 1953, Geology of Beaver Creek and adjacent areas, Utah: Salt Lake City, University of Utah, M.S. thesis, 54 p., 2 separate plates, scale 1:31,680.
- McKee, E.D., 1969, Paleozoic rocks of the Grand Canyon, in Baars, D.L., editor, Geology and natural history of the Grand Canyon region: Four Corners Geological Society, 5th Field Conference, Powell Centennial River Expedition, p. 78–90.
- Miall, A.D., 1978, Lithofacies types and vertical profile models in braided river deposits—a summary, in Miall, A.D., editor, Fluvial sedimentology: Canadian Society of Petroleum Geologists Memoir 5, p. 597–604.
- Morgan, C.D., 1993, Mississippian Leadville Limestone, in Hjellming, C.A., editor, Atlas of major Rocky Mountain gas reservoirs: New Mexico Bureau of Mines and Mineral Resources, p. 94.
- Parker, J.W., and Roberts, J.W., 1963, Devonian and Mississippian stratigraphy of the central part of the Colorado Plateau, in Bass, R.O., editor, Shelf carbonates of the Paradox Basin: Four Corners Geological Society, 4th Field Conference Guidebook, p. 31–60.
- Petroleum Information, 1984, Paradox Basin—unravelling the mystery: *Petroleum Frontiers*, v. 1, no. 4, p. 22.
- Sadlick, W., 1955, The Mississippian-Pennsylvanian boundary in

- northeastern Utah: Salt Lake City, University of Utah, M.S. thesis, 77 p.
- Sadlick, W., 1957, Regional relations of Carboniferous rocks of northeastern Utah, *in* Seal, O.G., editor, Guidebook to the geology of the Uinta Basin: Intermountain Association of Petroleum Geologists 8th Annual Field Conference, p. 57–77.
- Sandberg, C.A., and Gutschick, R.C., 1980, Sedimentation and biostratigraphy of Osagean and Meramecian starved basin and foreslope of the western United States, *in* Fouch, T.D., and Magathan, E.R., editors, Paleozoic paleogeography of the west-central United States-Rocky Mountain symposium 1: Rocky Mountain Section, Society of Economic Paleontologist and Mineralogists (Society for Sedimentary Geology), p. 129–147.
- Smith, L.B., 2004, Hydrothermal alteration of carbonate reservoirs—how common is it? [abs.]: American Association of Petroleum Geologists Annual Convention, Official Program with Abstracts, v. 13, p. A130.
- Smith, L.B. Jr., 2006, Origin and reservoir characteristics of Upper Ordovician Trenton—Black River hydrothermal dolomite reservoirs in New York: American Association of Petroleum Geologists Bulletin Special Issue—Hydrothermally Altered Carbonate Reservoirs, v. 90, no. 11, p. 1691–1718.
- Smith, L.B., Jr. and Davies, G.R., 2006, Structurally controlled hydrothermal alteration of carbonate reservoirs—introduction: American Association of Petroleum Geologists Bulletin Special Issue—Hydrothermally Altered Carbonate Reservoirs, v. 90, no. 11, p. 1635–1640.
- Smith, K.T., and Prather, O.E., 1981, Lisbon field—lessons in exploration, *in* Wiegand, D.L., editor, Geology of the Paradox Basin: Rocky Mountain Association of Geologists Guidebook, p. 55–59.
- Smouse, DeForrest, 1993, Lisbon, *in* Hill, B.G., and Bereskin, S.R., editors, Oil and gas fields of Utah: Utah Geological Association Publication 22, non-paginated.
- Spangler, L.E., 2005, Geology and karst hydrology of the eastern Uinta Mountains—an overview, *in* Dehler, C.M., Pederson, J.L., Sprinkel, D.A., and Kowallis, B.J., editors, Uinta Mountain Geology: Utah Geological Association Publication 33, p. 201–214.
- Sprinkel, D.A., 2006, Interim geologic map of the Dutch John 30' x 60' quadrangle, Daggett and Uintah Counties, Utah, Moffat County, Colorado, and Sweetwater County, Wyoming: Utah Geological Survey Open-File Report 491DM, compact disc, GIS data, 3 plates, scale 1:100,000.
- Sprinkel, D.A., 2007, Interim geologic map of the Vernal 30' x 60' quadrangle, Uintah and Duchesne Counties, Utah, Moffat and Rio Blanco Counties, Colorado: Utah Geological Survey Open-File Report 506DM, compact disc, GIS data, 3 plates, scale 1:100,000.
- Sprinkel, D.A., 2018, Interim geologic map of the Duchesne 30' x 60' quadrangle, Duchesne and Wasatch Counties, Utah: Utah Geological Survey Open-File Report 689, 37 p., 2 plates, scale 1:62,500.
- Swennen, R., Vandeginste, V., and Ellam, R., 2003, Genesis of zebra dolomites (Cathedral Formation—Canadian Cordillera fold and thrust belt, British Columbia): Journal of Geochemical Exploration, v. 78–79, p. 571–577.
- Utah Division of Oil, Gas and Mining, 2020, Oil and gas production report by field, December 2019: Online, <https://oilgas.ogm.utah.gov/oilgasweb/publications/monthly-rpts-by fld.xhtml?rptType=FLD>, accessed May 2020.
- Wallace, M., and Hood, A., 2018, Zebra textures in carbonate rocks—fractures produced by the force of crystallization during mineral replacement: Sedimentary Geology, v. 368, no. 3, doi:10.1016/j.sedgeo.2018.03.009.
- Welsh, J.E., and Bissell, H.J., 1979, The Mississippian and Pennsylvanian (Carboniferous) Systems in the United States—Utah: U.S. Geological Survey Professional Paper 1110-Y, 35 p.
- Wilson, J.L., 1975, Carbonate facies in geologic history: New York, Springer-Verlag, 471 p.